

1 **Isotopic paleoecology ( $\delta^{13}\text{C}$ ,  $\delta^{18}\text{O}$ ) of late Quaternary herbivorous mammal 2**  
3 **assemblages from southwestern Amazon**

3

4 Lidiane Asevedo<sup>1,2\*</sup>, Alceu Ranzi<sup>3</sup>, Risto Kalliola<sup>4</sup>, Martti Parssinen<sup>5</sup>, Kalle

5 Ruokolainen<sup>6</sup>, Mário Alberto Cozzuol<sup>7</sup>, Ednair Rodrigues do Nascimento<sup>8</sup>, Francisco

6 Ricardo Negri<sup>9</sup>, Jonas de Souza Pereira Filho<sup>3</sup>, Alexander Cherkinsky<sup>10</sup>, Mário André

7 Trindade Dantas<sup>1,2</sup>

8

9 *<sup>1</sup>Programa de Pós-graduação em Ecologia e Conservação, PPEC, Universidade Federal*  
10 *de Sergipe, São Cristóvão, Sergipe, Brazil. lidi.asevedo@gmail.com*

11 *<sup>2</sup>Laboratório de Ecologia e Geociências, Instituto Multidisciplinar em Saúde,*  
12 *Universidade Federal da Bahia, Vitória da Conquista, Bahia,*  
13 *Brazil.matdantas@yahoo.com.br*

14 *<sup>3</sup>Laboratório de Pesquisas Paleontológicas, Departamento de Ciências da Natureza,*  
15 *Universidade Federal do Acre, Rio Branco, Acre, Brazil. alceuranzi@hotmail.com,*  
16 *jpdesouzafilho@hotmail.com*

17 *<sup>4</sup>Department of Geography and Geology, University of Turku, Turku, Finland.*  
18 *riskall@utu.fi*

19 *<sup>5</sup>Department of World Cultures, University of Helsinki, Helsinki, Finland.*  
20 *martti.parssinen@helsinki.fi*

21 *<sup>6</sup>Department of Biology, University of Turku, Turku, Finland. kalle.ruokolainen@utu.fi*

22 *<sup>7</sup>Universidade Federal de Minas Gerais, Departamento de Zoologia, Belo Horizonte,*  
23 *Minas Gerais, Brazil. cozzuol@icb.ufmg.br*

24 *<sup>8</sup>Museu Estadual de Rondônia, Porto Velho, Rondônia, Brazil.*  
25 *ednair.nascimento@gmail.com*

26 <sup>9</sup>Laboratório de Paleontologia, Universidade Federal do Acre, Campus Floresta,  
27 Cruzeiro do Sul, Acre, Brazil. frnegri@bol.com.br

28 <sup>10</sup> Center for Applied Isotope Studies, University of Georgia, Athens, United States.  
29 acherkin@uga.edu

30

31 \*Corresponding author: L. Asevedo

32

### 33 **Abstract**

34 We report the first <sup>14</sup>C AMS datings and carbon ( $\delta^{13}\text{C}$ ) and oxygen ( $\delta^{18}\text{O}$ ) stable isotopes  
35 data to reconstruct the paleoecology of medium to large herbivorous mammals from late  
36 Quaternary of southwestern Amazon (Acre and Rondônia states, Brazil). AMS <sup>14</sup>C  
37 datings for *Neochoceros* sp. (29,072 - 27,713 Cal yr BP), *Notiomastodon platensis* (25,454  
38 - 24,884 Cal yr BP) and *Eremotherium laurillardii* (11,320 - 11,131 Cal yr BP) supports  
39 the Lujanian ages. All fossils have low  $\delta^{13}\text{C}$  and  $\delta^{18}\text{O}$  isotopic values that suggest  
40 heterogenous forest habitats, agreeing with paleovegetation reconstitution. Most species  
41 were browsers ( $p_i\text{C}_3 = 100\%$ ; Niche breadth,  $B_A = 0$ ), where the key species with the  
42 largest body mass, *N. platensis* (~6,300 kg) and *E. laurillardii* (~3,500 kg), possibly had  
43 a more generalized browser diet in closed-canopies to woodlands. Their diet distinguished  
44 from the  $\text{C}_3/\text{C}_4$  generalist *Trigodonops lopesi* (~1,900 kg), which foraged in wooded  
45 savannas ( $p_i\text{C}_3 = 70\%$ ;  $B_A = 0.72$ ), similarly with its relative *Toxodon platensis* (~1,800  
46 kg) that had a browse-dominated mixed feeder diet ( $p_i\text{C}_3 \geq 84\%$ ,  $B_A \leq 0.38$ ) in other  
47 localities of Amazonia. *Palaeolama major* (~280 kg) was possibly a strictly folivorous  
48 within subcanopies, whereas *Tapirus* sp. (~250 kg) and *Mazama* sp. (~40 kg) were  
49 browsers in subcanopies to woodlands. *Holmesina rondoniensis* (~120 kg) was a browser  
50 but not restricted, where could also feed on herbaceous from understories in woodlands,

51 and *Neochoerus* sp. (~ 200 kg) feeding predominantly herbaceous plants in wooded  
52 savannas ( $\delta^{13}C_3 = \sim 69\%$ ;  $B_A = 0.75$ ). We estimate that the interspecific competition could  
53 have been avoid by different feeding strategies, although more investigations are still  
54 needed to better understand their ecological interactions in the habitats of the  
55 southwestern Amazon during the late Quaternary.

56

## 57 **Keywords**

58 Pleistocene, Amazon, megafauna, paleodiet, stable isotopes, AMS  $^{14}C$  dating

59

## 60 **1. Introduction**

61 An emblematic Pleistocene fauna of herbivorous mammals is recognized in  
62 southwestern Amazon (Simpson and Paula Couto, 1981; Paula Couto, 1982, 1983a,  
63 1983b; Ranzi, 2000; Nascimento, 2008; Ranzi, 2008). The native notoungulates,  
64 cingulates, pilosans, caviids and also the Holartic immigrants, such as proboscideans,  
65 cetartiodactyls and perissodactyls are the most significant Quaternary members in this  
66 region (Ranzi, 2000; Góis et al., 2004; Porto et al., 2004; Holanda and Cozzuol, 2006;  
67 Nascimento, 2008; Ranzi, 2008; Holanda et al., 2011).

68 The first fossil occurrences have been reported at the beginning of the 20th century  
69 from alluvial Quaternary deposits outcropping along the banks of the Juruá River, affluent  
70 of the Amazon River in the states of Acre and Amazonas, Brazil (Simpson and Paula  
71 Couto, 1981; Ranzi, 2000, 2008). However, the knowledge about the Pleistocene  
72 mammal fossils from Rondônia state began in the 1980s, after the beginning of intense  
73 gold mining activity in the alluvial deposits of the Madeira River, also tributary of the  
74 Amazon River (Nascimento, 2008; Holanda et al., 2011).

75 Despite the great faunistic diversity, there are few inferences regarding the  
76 paleoecology of these assemblages. Ranzi (2000) assessed the ecological importance of  
77 the Pleistocene fauna from Juruá River in a comparative study with modern species,  
78 although no specific method for paleoecological fauna reconstruction has been performed.

79 The most traditional studies for paleoecological reconstructions use morphological  
80 inferences through analyses of dental hypsodonty, enamel microwear and mesowear,  
81 cranial shape adaptations, among others (e.g., Fortelius and Solounias, 2000; Solounias  
82 and Semprebon, 2002; Bargo et al., 2006; Naples and McAfee, 2012). Other studies  
83 retrieve direct evidence of the food content ingested through analysis of plant microfossils  
84 extracted from dental calculi and coprolites (e.g. Marcolino, 2012; Asevedo et al., 2012;  
85 2020). Nevertheless, increasing number of studies are employing isotopic analysis of  
86 fossilized mammalian mineralized tissues, proving to be an excellent tool (e.g., Sánchez  
87 et al., 2004; Macfadden, 2005; Domingo et al., 2012; Lopes et al., 2013; França et al.,  
88 2014; Dantas et al., 2013; 2017; Pansani et al., 2019).

89 The analysis of stable isotopes in paleoecology is based on the natural variation of  
90 stable isotope composition in animals (Fricke, 2007; Koch, 2007; Higgins, 2018).  
91 Ingestion of water and food along with the physiological processes of each animal leave  
92 a geochemical impression on the inorganic (bioapatite) and organic (collagen)  
93 components of its bones and teeth (Koch, 2007). Stable isotopes of carbon in mineralized  
94 mammal tissues are derived from their food, and are closely related to the photosynthetic  
95 pathways used by the plants consumed (Fricke, 2007; Koch, 2007; Marshall et al., 2007).  
96 On the other hand, the stable isotope of oxygen is mainly derived from the water ingested  
97 by drinking and food, and accordingly brings important inferences related to climatic  
98 factors (e.g., precipitation and temperature) of the species habitats (Sponheimer and Lee-  
99 Thorp, 1999; Fricke, 2007; Koch, 2007). Therefore, the analysis of carbon and oxygen

100 isotopes is important to identify feeding preferences and paleoenvironment of extinct  
101 mammals, as isotopic compositions vary with diet, location and ecosystem (Fricke, 2007;  
102 Koch, 2007; Higgins, 2018).

103 The present study provides a reconstruction of the paleoecology of medium to large  
104 herbivorous mammal assemblages from late Quaternary of southwestern Amazon  
105 through stable carbon and oxygen isotope analyses, and also supplying: (i)  $^{14}\text{C}$  datings by  
106 accelerator mass spectrometry (AMS) to contextualize the fossil assemblages, (ii)  
107 inferences about the paleoenvironment, and (iii) ancient diet and niche partitioning.

108

## 109 **2. Material and methods**

### 110 2.1. Samples

111 Eighteen bulk samples of enamel, dentin and bones were collected from species of  
112 Pilosa (Megatheriidae: *Eremotherium laurillardii* Lund, 1842), Cingulata  
113 (Pampatheriidae: *Holmesina rondoniensis* Góis et al., 2012), Proboscidea  
114 (Gomphotheriidae: *Notiomastodon platensis* Ameghino, 1888), Notoungulata  
115 (Toxodontidae: *Trigodonops lopesi* Roxo, 1921), Perissodactyla (Tapiridae: *Tapirus* sp.  
116 Brisson, 1762), Cetartiodactyla (Camelidae: *Palaeolama major* Liais, 1872 and Cervidae:  
117 *Mazama* sp. Rafinesque, 1817) and Rodentia (Caviidae: *Nechoerus* sp. Hay, 1926)  
118 (Supplementary Table 1). These samples were analyzed to obtain stable carbon and  
119 oxygen isotope composition from carbonate component of the bioapatite. AMS  $^{14}\text{C}$   
120 datings were performed for *E. laurillardii*, *N. platensis* and *Nechoerus* sp. samples, and  
121 were calibrated into calendar ages before present using CALIB 7.1 program (Reimer et  
122 al., 2013). Both analyses were performed at the Center for Applied Isotope Studies  
123 (CAIS) of the University of Georgia, United States.

124 The fossil specimens came from Quaternary alluvial deposits in several localities  
125 in the southwestern Amazon of the Upper Juruá (8°47'S - 9°49'S, 72°41'W - 72°49'W;  
126 Fig 1, locality 1, a-d) and Chandless rivers (9°49'50"S, 70°08'31"W, Fig. 1, locality 2)  
127 in Acre state, as also in Araras locality, Madeira River (10°03'01"S, 65°19'31"W; Fig.  
128 1, locality 3), Rondônia state, Brazil. The specimens are deposited in the paleontological  
129 collections of the Laboratório de Pesquisas Paleontológicas of Universidade Federal do  
130 Acre (LPP/UFAC), Rio Branco, Acre and the Museu da Memória Rondoniense (MERO),  
131 Porto Velho, Rondônia, Brazil.

132 Previous data of stable carbon and oxygen isotopes of the Toxodontidae *Toxodon*  
133 *platensis* Owen, 1840 from southwestern Amazon in Peru (8°24'S - 12°38'S, 71°18'W -  
134 74°17'W) and Bolivia localities (11°00'S - 14°01'S, 65°06'W - 69°00'W; Fig. 1,  
135 localities 4 - 9; Supplementary Table 1) by Macfadden (2005) were integrated into  
136 analysis in order to compare with the sympatric toxodontid *T. lopesi*, and also the other  
137 fossil taxa from Brazilian Amazonian localities.

138

## 139 2.2. Material processing

140 The stable isotope and AMS <sup>14</sup>C datings analyses followed the methodological steps  
141 of Cherkinsky (2009). Two cleaning steps were initially performed on the bone and tooth  
142 samples: first, a mechanical wash using an ultrasonic bath and wire brush to remove  
143 external material (i.e., dirt, secondary materials, etc), and second, a chemical cleaning to  
144 remove diagenetic carbon compounds. The materials were soaked overnight in 1N acetic  
145 acid, then washed free of acetic acid by repeated decantation. Loose or extraneous  
146 material was discarded and the samples were dried at approximately 70°C. After drying,  
147 samples were crushed into small fragments and again reacted with 1N acetic acid in a  
148 250-mL Erlenmeyer flask. The flask was periodically evacuated to remove air and/or CO<sub>2</sub>

149 from micropores, after which the flask is returned to atmospheric pressure to force fresh  
150 acid into microspaces of the sample. This process of evacuation and repressuring was  
151 performed at ~20-minute intervals until no substantial release of fine, foamy gas bubbles  
152 occurs, and it was repeated at least 4-5 times. Once the evolution of fine gas bubbles has  
153 ceased, it can be assumed that all secondary or surface-exchanged carbonates have been  
154 removed.

155 The completely cleaned bone samples were washed free of acetic acid by repeated  
156 soaking and decantation with demineralized water and then vacuum-dried with 100%  
157 phosphoric acid to dissolve the bone/tooth mineral and release carbon dioxide from  
158 hydroxyapatite. The resulting carbon dioxide was cryogenically purified from other  
159 reaction products and catalytically converted to graphite. The sample ratios were  
160 measured separately using a stable isotope ratio mass spectrometer.

161 All results are reported using delta notation,  $\delta = [(R_{\text{sample}}/R_{\text{standard}} - 1) \times 1000]$   
162 (Coplen, 1994). The reference for carbon isotope values ( $R = {}^{13}\text{C}/{}^{12}\text{C}$ ) is Vienna Pee Dee  
163 Belemnite (VPDB) and oxygen isotope ( $R = {}^{18}\text{O}/{}^{16}\text{O}$ ) is ~~the~~ Vienna Standard Mean Ocean  
164 Water (VSMOW).

165

### 166 2.3. Interpretation of $\delta^{13}\text{C}$ data

167 The interpretation of carbon isotope values found in tooth/bones of medium-to  
168 large-bodied herbivorous mammals are based on fractionated values of the plant  
169 photosynthetic pathway consumed (Fricke, 2007; Koch, 2007; Higgins, 2018). Plants  
170 have two main photosynthetic pathways,  $\text{C}_3$  and  $\text{C}_4$  (Ehleringer and Cerling, 2002).  $\text{C}_3$   
171 plants, which fix carbon using the Calvin Cycle, comprise ~85% of terrestrial plant  
172 biomass, encompassing most trees, shrubs, and grasses from high-elevation, high latitude,  
173 and cool-growing seasons. The  $\delta^{13}\text{C}$  values range from  $-35\text{‰}$  to  $-22\text{‰}$  with mean value

174 of  $-27\text{‰}$  (Koch, 2007; Marshall et al., 2007). Values of  $\delta^{13}\text{C}$  below  $-30\text{‰}$  reflect  $\text{C}_3$   
175 plants from closed-canopy forest environments, whereas values close to the limit of  $\text{C}_3$   
176 plants may be associated with  $\text{C}_3$  grasslands (e.g.,  $-23$  to  $-22\text{‰}$ ; Kohn, 2010).  $\text{C}_4$  plants,  
177 in turn, fix carbon using the Hatch-Slack cycle and comprise about 5-10% of the terrestrial  
178 plant biomass, including predominantly grasses, herbs and eudicotyledons adapted to arid  
179 and high luminosity index environments (Ehleringer and Cerling, 2002). The  $\delta^{13}\text{C}$  values  
180 range from  $-17\text{‰}$  to  $-9\text{‰}$  and the mean value is  $-13\text{‰}$  (Koch, 2007; Marshall et al.,  
181 2007).

182 Consumers are enriched in  $^{13}\text{C}$  compared to the plants. Previous studies  
183 demonstrated that medium-to large-bodied herbivorous mammals had an enrichment of  
184 around  $14\text{‰}$  ( $\epsilon^*$  bioapatite-diet; Cerling and Harris, 1999). However, recently, Tejada-  
185 Lara et al. (2018) suggested that the body mass (bm) influences the physiological carbon  
186 enrichment values, and their determination should be calculated based on an equation:  $\epsilon^*$   
187  $= 2.4 + 0.034 (\text{bm})$ .

188 In spite of the body mass estimates for extinct species that do not have living  
189 relatives are approximations and vary in literature, it was considered the most recent  
190 published data to integrate in the analysis (i.e., Ghizzoni, 2014; Dantas, 2019; Dantas et  
191 al., 2020; Table 1). For the fossils of extant taxa, *Tapirus* sp. and *Mazama* sp., we  
192 followed the body mass data of the most common species of the respective genera in the  
193 Amazon region, *Tapirus terrestris* Linnaeus, 1758 (i.e., Padilla and Dowler, 1994) and  
194 *Mazama americana* Erxleben, 1777 (i.e., Duarte and Jorge, 1996; Table 1). Through these  
195 data, it was calculated an enrichment of  $12\text{‰}$  for taxon with body mass less than 75 kg,  
196  $13\text{‰}$  for those species between 75 kg to 600 kg,  $14\text{‰}$  between 600 kg to 3,500 kg, and  
197  $15\text{‰}$  for species as from 3,500 kg.



198           Accordingly, diet categories based on the digestive physiology of herbivores can be  
199 discerned between browsers, grazers and mixed feeders. Browser mammals consume  
200 larger proportions of fruit and foliage from C<sub>3</sub> shrub and tree plants (Fricke, 2007; Koch,  
201 2007; Higgins, 2018), and based on the different enrichments in bioapatite (i.e., 15‰ to  
202 12‰), they have average δ<sup>13</sup>C values of – 12‰ to – 15‰, respectively. Grazing mammals  
203 are consumers of herbs and grasses (Fricke, 2007; Koch, 2007; Higgins, 2018). C<sub>3</sub> grazers  
204 may have δ<sup>13</sup>C values approximately between – 8‰ to – 7‰ and – 11‰ to – 10‰,  
205 although it is still difficult to distinguish the diet between C<sub>3</sub> grasses and wood resources,  
206 due to the overlap in δ<sup>13</sup>C values for certain phytophysiognomies (e.g., C<sub>3</sub> grassland and  
207 wooded savanna). On the other hand, C<sub>4</sub> grazers have specific average δ<sup>13</sup>C values of 2‰  
208 to –1‰. Mixed feeder species that consume both browse and grass (C<sub>3</sub>-C<sub>4</sub>), have  
209 intermediate values between the average of browsers and C<sub>4</sub> grazers (– 12‰ to – 15‰  
210 and 2‰ to –1‰).

211           In order to identify the landscape characteristics of mammalian fossil habitats, we  
212 used the interpretation of the δ<sup>13</sup>C ranges from Domingo et al. (2012) following the  
213 specific enrichment values. Therefore, species from (i) closed-canopy forest habitats [i.e.,  
214 higher density areas of trees forming canopy] have values from – 20‰ and – 15‰ to –  
215 23‰ and – 18‰; (ii) mesic woodland habitats [i.e., low-density forest with sparse  
216 understory plants] have values from – 15‰ and – 10‰ to – 18‰ and – 13‰; (iii) wooded  
217 C<sub>3</sub> grassland [i.e., arboreal savannas] have values from – 10‰ and – 7‰ to – 13‰ and –  
218 10‰; (iv) mixed C<sub>3</sub> and C<sub>4</sub> habitats [i.e., arboreal savannas] have values from – 7‰ and  
219 – 2‰ to – 10‰ and – 5‰; and (iv) open C<sub>4</sub> grassland habitats [i.e., open savannas] have  
220 values from – 2‰ and 6‰ to – 5‰ and 3‰.

221           Comparisons between carbon isotope values of the fossil taxa and the living related  
222 species from the literature were performed taking into account the enrichment addition of

223 2‰ to the extant species, because of the  $\delta^{13}\text{C}$  decay of atmospheric  $\text{CO}_2$  in current  
 224 ecosystems (Suess effect), as a consequence of the large burning of fossil fuels since the  
 225 beginning of the Industrial Revolution in the 18th century (Keeling, 1979). Previous data  
 226 of stable carbon isotopes analyzed in collagen samples from current species were  
 227 converted to bioapatite values. Herbivorous mammal collagen is known to be 5‰  
 228 enriched in relation to the food (Koch, 2007). Thus, following Tejada-Lara (2018), from  
 229 the  $\delta^{13}\text{C}$  value of the resource found ( $\delta^{13}\text{C}_{\text{collagen}} - 5\text{‰}$ ) was added the specific enrichment  
 230 values for bioapatite according to the body mass of the species.

231

### 232 2.3.1. Diet proportions and ecological niches estimates

233 In order to refine the diet interpretations, the  $\delta^{13}\text{C}$  data and respective enrichment  
 234 values considered for each taxon were used to calculate the proportion of  $\text{C}_3$  and  $\text{C}_4$  diet  
 235 for the species, using the following equation presented by Phillips (2012):

$$236 \quad (1) \quad \delta^{13}\text{C}_{\text{mix}} = \delta^{13}\text{C}_1 f_1 + \delta^{13}\text{C}_2 f_2$$

$$237 \quad (2) \quad 1 = f_1 + f_2$$

238 Where,  $\text{C}$  represents the mean  $\delta^{13}\text{C}$  values of  $\text{C}_3$  ( $\text{C}_1 = -12\text{‰}$  to  $-15\text{‰}$ ) and  $\text{C}_4$   
 239 ( $\text{C}_2 = 2\text{‰}$  to  $-1\text{‰}$ ) plant consumers.  $f_1$  and  $f_2$  are the proportion of  $\text{C}_3$  and  $\text{C}_4$  resources,  
 240 respectively.

241 Through the values obtained from the proportion of resources it was possible to  
 242 calculate the ecological niche breadth according to the following Pianka (1973)  
 243 equation:

$$244 \quad B = 1 / \sum p_i^2$$

245 Where,  $B$  is the niche breadth and  $p_i$  the proportion of resources consumed.

246 This measure was then standardized from 0 to 1 following the equation of Levins (1968):

$$247 \quad B_A = B - 1/n - 1$$

248           Where,  $B_A$  is standardized niche width,  $B$  is the niche breadth, and  $n$  is the number  
249 of resources consumed. The results indicate whether the animal is specialist (0) or  
250 generalist (1)

251

#### 252 2.4. Interpretation of $\delta^{18}\text{O}$ data

253           The stable isotope of oxygen in mammalian bioapatite is directly related to their  
254 body water. It reflects the oxygen isotope composition that enters in organism through  
255 atmospheric  $\text{O}_2$ , ingested water and food sources, and exits via respiration, transpiration  
256 and excretion. Thereby, resulting in a complex function of climate, diet and physiology  
257 (Sponheimer and Lee-Thorp, 1999; Koch, 2007).

258           Since the  $\delta^{18}\text{O}$  values of atmospheric  $\text{O}_2$  are relatively constant, large herbivorous  
259 mammals that require considerable amount of ingested water from lakes and rivers, have  
260  $\delta^{18}\text{O}$  values reflecting the response of meteoric water ( $\delta^{18}\text{O}_{\text{mw}}$ ) to changes in temperature  
261 and/or precipitation/humidity (Sponheimer and Lee-Thorp, 1999; Fricke, 2007; Koch,  
262 2007), which can be influenced geographically and temporally by several climatic factors  
263 (e.g., continentality, latitude, altitude, amount effect, among others; Sponheimer and Lee-  
264 Thorp, 1999; MacFadden and Higgins 2004; Koch, 2007; Higgins, 2018).

265           Traditionally, in terrestrial ecosystems the more positive  $\delta^{18}\text{O}$  values in mammal  
266 tissues are indicative of warmer and/or drier habitats/seasons, due to the  $^{18}\text{O}$ -enrichment  
267 in detriment of the higher  $^{16}\text{O}$ -evapotranspiration in ingested waters and plants  
268 (Sponheimer and Lee-Thorp, 1999; Fricke, 2007; Koch, 2007). The evapotranspiration  
269 effect is larger in  $\text{C}_4$  plants that do not close their stomata, and consequently grazer  
270 mammals have the most enriched  $\delta^{18}\text{O}$  values (Fricke, 2007; Koch, 2007). On the other  
271 hand, negative  $\delta^{18}\text{O}$  values may reflect a colder and/or wetter habitats/seasons, which  
272 contributes to depletion of  $^{18}\text{O}$  from water surfaces and plants (Sponheimer and Lee-

273 Thorp, 1999; Fricke, 2007; Koch, 2007). Specifically, in tropical forested habitats, the  
274 reduction of  $^{16}\text{O}$  evapotranspiration in  $\text{C}_3$  plants adapted to shaded environments, plus the  
275 amount effect that cause a depression in the oxygen isotopic curves related to the high  
276 precipitation may favors the depletion in  $\delta^{18}\text{O}$  values for browser mammals (MacFadden  
277 and Higgins 2004; Fricke, 2007; Koch, 2007; Higgins, 2018).

278 Mammal species inhabiting similar environments can also vary their  $\delta^{18}\text{O}$  data in  
279 response to different proportion of drinking water surfaces as opposed to plant water  
280 consumptions (Sponheimer and Lee-Thorp, 1999; Levin et al., 2006). Some herbivorous  
281 mammals get most of their water from plants, and have the  $\delta^{18}\text{O}$  values reflecting not only  
282 the local precipitation, but also the local environmental relative humidity that control the  
283  $^{18}\text{O}$  enrichment in plants (Ayliffe et al., 1992). These taxa are sensitive to changes in  $\delta^{18}\text{O}$   
284 values with increased aridity (evaporation-sensitive), differing to those taxa that are  
285 obligatory drinkers (evaporation-insensitive; Levin et al., 2006).

286

#### 287 2.4.1. Estimation of $\delta^{18}\text{O}$ in ancient environmental waters

288 The oxygen values in bioapatite of obligatory drinkers can be used as a proxy to  
289 past meteoric water  $\delta^{18}\text{O}$  estimation. Such relationship is consistent with the relationship  
290 between measured phosphate  $\delta^{18}\text{O}$  values ( $^{18}\text{Op}$ ) of bones and teeth of modern African 291  
(*Loxodonta africana* Blumenbach, 1797) and Asian (*Elephas maximus* Linnaeus, 1758)  
292 elephants and estimates of  $^{18}\text{O}_{\text{mw}}$  (Ayliffe et al., 1992). Thus, assuming modern elephants  
293 are a reasonable analog for the South American proboscidean *N. platensis*, we converted  
294 its isotopic values from bioapatite carbonate ( $\delta^{18}\text{Oc}$ ) to phosphate values ( $\delta^{18}\text{Op}$ ) by  
295 reducing the  $\delta^{18}\text{Oc}$  values to 8.7‰ (Bryant et al., 1996). Posteriorly, it was calculated the  
296  $\delta^{18}\text{O}_{\text{mw}}$  of *N. platensis* using the relationship between the oxygen content of the  $\text{PO}_4$

297 component of bioapatite ( $\delta^{18}\text{Op}$ ) and ingested water in modern elephants through the  
298 equation of Ayliffe et al. (1992):

$$299 \quad \delta^{18}\text{Op} = 0.94\delta^{18}\text{O}_{\text{mw}} + 23.3$$

300

### 301 **3. Results**

302 The  $^{14}\text{C}$  AMS datings indicate that the specimens are biostratigraphically correlated  
303 to the Lujanian Stage/Age (SALMA), and include similar ages for *Neochoerus* sp.  
304 (29,072 - 27,713 cal yr BP) and *N. platensis* (25,454 - 24,884 cal yr BP) from Madeira  
305 and Juruá rivers in Rondônia and Acre states, respectively. Furthermore, a more recent  
306 age was obtained for *E. laurillardi* (11,320 - 11,131 cal yr BP) from the Chandless River,  
307 Acre state (Supplementary Table 1).

308 The low  $\delta^{13}\text{C}$  values obtained from bioapatite in mammals from the southwestern  
309 Amazon Pleistocene mammals ( $-17.47\text{‰}$  to  $-8.83\text{‰}$ ; Supplementary Table 1), indicate  
310 a tendency toward a  $\text{C}_3$  specialist diet ( $p_{\text{C}_3} = 100\%$ ;  $B_A = 0$ ) from closed-canopy forest  
311 to wooded  $\text{C}_3$  grasslands (Table 1; Fig. 2).

312 The largest bodied species *N. platensis* (bm:  $\sim 6,300$  kg) and *E. laurillardi* (bm:  $\sim$   
313 3,500 kg) have  $\delta^{13}\text{C}$  values below the average of  $-12 \text{‰}$  for  $\text{C}_3$  diet, which indicate  
314 browsing diet in more closed physiognomies (Fig. 2A). *E. laurillardi* possibly inhabited  
315 closed-canopy forests in Acre (Juruá River:  $-17.04 \pm 0.20 \text{‰}$ ; Chandlers River:  $-15.37$   
316  $\text{‰}$ ) and mesic woodlands in Rondônia ( $-14.23\text{‰}$ ; Table 1). *N. platensis*, in turn, has a  
317 slightly broad range of  $\delta^{13}\text{C}$  values and inhabited closed-canopy forests and mesic  
318 woodlands in both localities of Acre ( $-14.11 \pm 2.4 \text{‰}$ ) and Rondônia ( $-15.09 \pm 1.16 \text{‰}$ ;  
319 Table 1; Fig. 2A).

320 Among the species with the highest body mass, the notoungulate *T. lopesi* (bm:  $\sim$   
321 1,900 kg) of Rondônia has a  $\delta^{13}\text{C}$  value significantly more positive ( $-8.83 \text{‰}$ ; Table 1),

322 indicative of mixed feeder ( $B_A = 0.72$ ) in wooded savanna-like habitats with dominant  $C_3$   
323 plants ( $p_iC_3 = 70\%$ ; Table 1; Fig. 2B). For the sympatric toxodontid *T. platensis* (bm: ~  
324 1,800 kg) from southwestern Amazon localities in Bolivia ( $-13.9 \pm 1.6\%$ ;  $p_iC_3 \geq 86\%$ ,  
325  $B_A \leq 0.32$ ) and Peru ( $-13.2 \pm 1.4\%$ ;  $p_iC_3 \geq 84\%$ ,  $B_A \leq 0.38$ ) by Macfadden (2005), the  
326  $\delta^{13}C$  values indicate browse-dominated mixed feeder habits in mesic woodlands to  
327 wooded  $C_3$  grasslands (Table 1; Fig. 2B).

328 For the mammal species with lower body mass, a more positive  $\delta^{13}C$  value was  
329 observed for the large capybara *Neochoerus* sp. (bm: ~ 200 kg) from Rondônia ( $-9.66$   
330  $\%$ ) close to the value found in the toxodont for the same region (Fig. 2). The species  
331 probably had a more generalist diet between  $C_3$  and  $C_4$  resources ( $B_A = 0.75$ ), accessing  
332 more open landscapes dominated by  $C_3$  plants ( $p_iC_3 = 69\%$ ; Table 1; Fig. 2C).

333 The other mammal species have  $\delta^{13}C$  values below the average of  $-14\%$  and  $-15$   
334  $\%$  ( $\epsilon^* = 13$  and  $12\%$ , respectively), and also pointed to specialist browser diet such as  
335 the ground sloth and the proboscidean (Fig. 2C). *Tapirus* sp. (bm: ~ 250 kg) probably was  
336 a browser in closed-canopy forests in Juruá River ( $-17.33\%$ ) and mesic woodlands in  
337 Rondônia ( $-14.77\%$ ; Table 1; Fig. 2C). The camelid *P. major* (bm: ~ 280 kg) was a  
338 browser in closed-canopy forest in Juruá River ( $-17.47\%$ ), and the pampatheriid *H.*  
339 *rondoniense* (bm: ~ 120 kg) and the cervid *Mazama* sp. (bm: ~ 40kg) were browsers in  
340 solely-mesic woodlands habitats in Rondônia ( $-14.89\%$  and  $-15.47\%$ , respectively;  
341 Table 1; Fig. 2C).

342 The  $\delta^{18}O$  values are constantly low for all the species (19.90 to 25.80  $\%$ ; Table 1;  
343 Supplementary Table 1; Fig. 2), indicating similar conditions in precipitation amount and  
344 degree of rainfall/transpiration for both forest and wooded savanna landscapes in  
345 localities of Acre and Rondônia states. The slightly  $\delta^{18}O$  variations may have been  
346 influenced by monsoonal climates (wet and dry seasons) affecting the  $\delta^{18}O$  values of

347 ingested water ( $\delta^{18}\text{O}_{\text{mw}}$ ). The  $\delta^{18}\text{O}_{\text{mw}}$  results for *N. platensis* point more  $^{18}\text{O}$ -depleted  
348 water sources around the Madeira River in Rondônia (mean =  $-9.50\text{‰} \pm 0.9\text{‰}$ ) compared  
349 to the localities of Juruá River in Acre (mean =  $-7.51\text{‰} \pm 0.5\text{‰}$ ; Table 2). It corroborates  
350 with the lowest  $\delta^{18}\text{O}$  values founded for the generalists *T. lopesi* and *Nechoerus* sp. also  
351 from Rondônia (20.29 ‰ and 19.90 ‰; Table 1; Fig. 2B and C). Their oxygen results  
352 plus the enriched  $\delta^{13}\text{C}$  values can indicate a more open habitats close to riverine resources.  
353 By contrast, the browser *P. major* from Acre, showed the highest  $\delta^{18}\text{O}$  value (25.80 ‰;  
354 Table 1; Fig. 2C), probably related to the consumption of more  $^{18}\text{O}$ -enriched water  
355 sources. Although, the more depleted  $\delta^{13}\text{C}$  values found in this camelid may also indicate  
356 a significant diet of foliage, and would explain the more positive oxygen value, because  
357 leaf water is more  $^{18}\text{O}$ -enriched.

358

#### 359 **4. Discussion**

##### 360 *4.1. Radiocarbon dating of mammal assemblages from southwestern Amazon*

361 The AMS  $^{14}\text{C}$  datings of the fossils indicate that the mammal assemblages from  
362 southwestern Amazon in Acre and Rondônia states are biostratigraphically correlated to  
363 the Lujanian Stage/Age SALMA. Late Pleistocene ages were obtained for Juruá and  
364 Madeira river records, which is in agreement to the chronological and biostratigraphy of  
365 fossiliferous deposits for both rivers ( $\sim 43$  to 29 ka BP and  $\sim > 46$  to 27 Ka BP,  
366 respectively; Latrubesse and Rancy, 1998; Rizzotto and Oliveira, 2005), whereas an early  
367 Holocene age was obtained for the new record in Chandless River, Acre.

368 The Pleistocene assemblages are also chronologically correlated to the fossil  
369 records of other river basins of western Amazonia, including the Ucayali River, Peru (40  
370 to 32 ka BP), Madre de Dios River, Peru (38 to 36 ka BP), and Caquetá River, Colombia  
371 (55 to 30 Ka BP; Latrubesse and Rancy, 1998).

372

373 4.2. *The habitat landscapes from late Quaternary of southwestern Amazon*

374 The isotopic carbon and oxygen signature of the late Quaternary mammals from  
375 Acre and Rondônia states, support that the paleocommunity would have inhabited C<sub>3</sub>-  
376 dominated environments, with species occurring from closed-canopies, mesic woodlands  
377 to wooded savannas (Fig. 3A-C). The suggested environmental heterogeneity also  
378 characterizes the modern landscapes of the southwestern Amazon, consisting of non-  
379 flooded "Terra Firme" and periodically flooded Várzea forests. The dominant regional  
380 physiognomy is composed of spaced trees with few dense shrubby strata (open  
381 ombrophilous forest), with floristic formations also composed of palm trees (e.g., *Attalea*  
382 *speciosa*), bamboos (e.g., *Guadua superba*) and sororocas (e.g., *Phenakospermum*  
383 *guianensis*). Closed canopy forests (dense ombrophilous forests) to open ones  
384 conditioned by climate seasonality (semideciduous seasonal forests), mixed forest and  
385 grassy-woody vegetation (campinaranas), and forested savannas also configure the  
386 current physioecological zones of this rich Amazon region (IBGE, 2012).

387 The paleoenvironmental interpretation of the late Quaternary in Amazonia is an  
388 issue still debated. Many paleoenvironmental reconstructions suggest that the distribution  
389 of the Amazonian rainforest has changed mainly due to climatic fluctuations during  
390 glacial/interglacial events. As consequence, it was proposed alternating periods of forest  
391 contraction forming refuge regions followed by its expansion during distinct dry and wet  
392 conditions (Haffer, 1969; Liu and Colinvaux, 1985; Bush et al., 1990; Colinvaux et al.,  
393 1996; Ledru, 2002; Ledru et al., 2006), savanna corridors during Last Glaciation (van der  
394 Hammen and Hooghiemstra, 2000), as well as retractions of equatorial rain forests  
395 associate to expansion of tropical ones (similar to Atlantic forest; Arruda et al., 2017).  
396 Nevertheless, some studies do not support these changes in landscapes, and suggest a



397 paleoclimatic scenario relatively undisturbed for Amazonian rainforest during the last 50  
398 ka BP (Colinvaux et al., 1996, 2000, 2001; Bush et al., 2004; Irion et al., 2006; Mayle  
399 and Power, 2008).

400 The isotopic results of the mammalian fossils do not correspond with abrupt  
401 changes in the C<sub>3</sub> landscapes. The carbon and oxygen isotope values persist constantly  
402 low for all the specimens analyzed, including fossils of the glacial periods around ~ 30 to  
403 25 ka BP (<sup>14</sup>C results of *Neochoerus* sp and *N. platensis*, respectively), and of the  
404 beginning in interglacial period around ~11 ka BP (<sup>14</sup>C dating of *E. laurillardii*). These 405  
data are in concordance with the isotope data of *T. platensis* specimens from Amazonian  
406 localities in Peru and Bolivia with ages ranging from ~ 38 ka to 15 ka BP evaluated by  
407 Macfadden (2005).

408 These results corroborate with the humid climate conditions during the late glacial  
409 - early Holocene estimated for the southwestern Amazon. Specifically, in Rondônia state,  
410 palynological analysis indicate that forests were dominant in Katira creek around 55 ka  
411 to 26 ka BP (van der Hammen and Absy, 1994) and in Madeira Formation during 46 to  
412 27 ka BP (Rizzotto and Oliveira, 2005). Through isotopic, sedimentological and  
413 geomorphological analyses performed in a marginal area of Madeira river, Rossetti et al.  
414 (2017) also confirmed that the climate was wet and cold from 40 ka BP up to the Last  
415 Glaciation Maximum (LGM). Pollen data indicates the presence of cold-adapted plants  
416 (e.g., *Alnus*, *Hedyosmum*, *Weinmannia* and *Podocarpus*), which became absent in the  
417 Holocene, in association with herbs and tree taxa similar to modern ones (Cohen et al.  
418 2014).

419 During the LGM, the humidity was reduced and the temperature was between 2°  
420 and 6°C below modern values (van der Hammen and Absy 1994; van der Hammen and  
421 Hooghiemstra 2000; Cohen et al. 2014). Thus, an intensified aridity toward the end of the

422 late Pleistocene was estimated in Madeira river region (Rossetti et al., 2017), whereas  
423 savanna expansion was proposed for Katira site related to a dry climatic phase between  
424 26 to 13 ka BP (van der Hammen and Absy, 1994). On the other hand, in localities of  
425 Amazonas and Rondônia border, the carbon isotopes of soil organic matter suggest that  
426 these regions were still covered by forest vegetation between 17 to 9 ka BP (Freitas et al.,  
427 2001).

428 In spite of the carbon isotope results of *T. lopesi* and *Neochoerus* sp. from Rondônia  
429 indicating foraging in habitats with low proportion of C<sub>4</sub> plants (~30%), the isotopic  
430 signature consistently low for the most of the analyzed specimens do not support  
431 dominance of savanna habitats as previously inferred for the same assemblages in other  
432 studies (Latrubesse and Rancy, 1998; Ranzi, 2000; Ranzi, 2008). Ground sloths,  
433 proboscideans, toxodonts and cingulates were animals able to feeding on grasses, thus if  
434 the dry savanna habitats were present in southwestern Amazon, the carbon isotope values  
435 characteristic of C<sub>4</sub> plants would have been more significant. On the other hand, our data  
436 indicate that some species possibly were inhabiting closed canopy forests and consumed  
437 plants with carbon values below – 30‰. These values are seen in plants that are under the  
438 influence of the “canopy effect”, which produces <sup>13</sup>C-depleted and a gradient of leaf δ<sup>13</sup>C  
439 values from the ground (most negative values) to the canopy (van der Merwe and Medina,  
440 1991).

441 Furthermore, an interesting fossil record of *Guadua* sp. in Madre de Dios (Peru),  
442 which currently makes up extensive areas of bamboo forests in southwestern Amazonia,  
443 suggests that these forests were already present prior to the LGM (~ 3.12 ± 0.02 Ma and  
444 ~45 ka BP; Olivier et al., 2009), and that Pleistocene mammals could also have been  
445 accessed.

446 The depleted  $\delta^{18}\text{O}_{\text{mw}}$  of *N. platensis* reflects to the "continental and amount effects"  
447 that occurs in tropical amazon. Thus, it seems consistent with speleothem and stalagmite  
448 oxygen isotope data from western Amazonia. For Cueva Santiago in Amazonian Ecuador  
449 the results do not indicate prolonged drying during the last 95 ka ( $\delta^{18}\text{O} = -8.05$  to  $-4.52$   
450 ‰), and the climate condition during the LGM (23 ka and 19 ka BP) was wetter  
451 (Mosblech et al., 2012). Similarly, in El Condor and Cueva del Diamante caves, both  
452 located on the eastern flank of the Andes in northern Peru, indicate a wetter LGM and a  
453 drier early-mid Holocene in an opposite pattern to eastern Amazon (Cheng et al., 2013).

454 Based on oxygen isotopes in fluid inclusions from speleothems from Cueva del  
455 Tigre Perdido, in Peruvian Amazon, van Breukelen et al. (2008) proposed that the  
456 temperature change was small throughout the last ~13.5 ka BP, but the rainfall amount  
457 was reduced by 15–30% below present values. Thus, according to carbon isotopes of soil  
458 analysis the warmer and drier conditions could support savanna vegetation in Rondônia  
459 only during the early to middle Holocene, whereas during the late Holocene the moisture  
460 favored the expansion of the Amazonian rainforest as known today (Pessenda et al., 1998;  
461 Freitas et al., 2001). By contrast, any major shift of the forest vegetation toward open  
462 savanna was notified for the last 10 ka in the eastern Acre at Severino Calazans (Parssinen  
463 et al., in press).

464

#### 465 4.1.4.3. *Feeding ecology of the late Pleistocene mammals*

466 In the ancient assemblages of Amazon Quaternary mammals, most species were  
467 browsers feeding mostly on leaves and fruits of arboreal/scrub plants. The largest bodied  
468 species, *E. laurillardii* and *N. platensis*, probably occupied similar niches in southwestern  
469 Amazon, inhabiting from closed-canopy forests to mesic woodlands. The slightly wider  
470 range of carbon values for the proboscideans indicates a greater food plasticity (Fig. 4A

471 and B; Supplementary Table 1). *N. platensis* was an endemic proboscidean from South  
472 America, whose generalist diet was probably similar to the extant elephants. Diet  
473 followed habitat phytophysiognomy, and it consisted predominantly of herbaceous  
474 plants, foliar and floral branches, fruits and woody parts (Asevedo et al., 2012; 2020;  
475 Mothé et al., 2017). According to the carbon isotopes data, this proboscidean could have  
476 been a specialist C<sub>3</sub> browser in forest habitats of southwestern Amazon ( $\mu\delta^{13}\text{C} = -15.39$   
477  $\pm 1.63$  ‰; median: -15.61; IQR: -2.21; Fig. 4B), but was a browser or mixed feeder in C<sub>3</sub>  
478 woodlands/grasslands from Pampean regions of Argentina, Uruguay and Brazil ( $\mu\delta^{13}\text{C} =$   
479  $-8.2 \pm 2.1$  ‰; median: -8.26; IQR: -1.4; Fig. 4B; Sánchez et al., 2004; Gutiérrez et al.,  
480 2005; Domingo et al., 2012; Lopes et al., 2013), a dominant grazing diet in C<sub>4</sub> grasslands  
481 in the Brazilian Intertropical Region (BIR;  $\mu\delta^{13}\text{C} = -1.08 \pm 2.66$  ‰; median: -0.20; IQR:  
482 -1.78; Fig. 4B; Sánchez et al., 2004; Viana et al., 2011; Dantas et al., 2013; França et al.,  
483 2014; Dantas et al., 2017; Pansani et al., 2019), and a mixed feeding diet in C<sub>3</sub>-C<sub>4</sub>  
484 woodland/grassland landscapes in Andean regions of Ecuador and Peru ( $\mu\delta^{13}\text{C} = -4.7 \pm$   
485  $3.11$  ‰; median: -5.72; IQR: -6.45; Fig. 4B; Sánchez et al., 2004; Domingo et al., 2012),  
486 and also in Argentinean Chaco ( $\mu\delta^{13}\text{C} = -4.8 \pm 3.27$  ‰; median: -4.63; IQR: -5.58; Fig.  
487 4B; Alberdi et al., 2008; Domingo et al., 2012).

488 With a Pan-American distribution covering the southeastern North America to  
489 southern Brazil, the ground sloth *E. laurillardii* has also been estimated as a generalist  
490 species (Dantas et al., 2017). The carbon isotope analysis in specimens of the BIR  
491 demonstrated a large range that covers pure C<sub>3</sub> (browser), mixed feeders and pure C<sub>4</sub>  
492 (grazer) consumers ( $\mu\delta^{13}\text{C} = -5.4 \pm 3.92$  ‰; median: -5.11; IQR: -4.54; Fig. 4A; Viana  
493 et al., 2011; Dantas et al., 2013, 2014; França et al., 2014; Dantas et al., 2017; Pansani et  
494 al., 2019), differing from our results for an exclusive C<sub>3</sub> browser pattern in the Brazilian  
495 Amazon ( $\mu\delta^{13}\text{C} = -15.92 \pm 1.38$  ‰; median: -16.14; IQR: -2.60; Fig. 4A).

496 The reconstruction of the cranial musculature of *E. laurillardi* by Naples and  
497 McAfee (2012) suggested a masticatory pattern that could increase in efficiency for each  
498 chewing cycle. The high ability of oral processing related to the low digestive efficiency  
499 was suggested for the other American giant sloth species, *Megatherium Americanum*  
500 (Bargo et al., 2006). This species that had a similar biomechanical apparatus compared to  
501 *E. laurillardi*, probably was a generalized selective feeder, capable of consuming a variety  
502 of turgid or moderate to soft tough and abrasive food items (Oliveira et al., 2020). *E.*  
503 *laurillardi* would be able to browse on small branches, leaves, and fruits and possibly had  
504 a more selective diet in Amazonian localities than *N. platensis*.

505 On the other hand, the toxodonts, especially *T. lopesi*, have the highest ecological  
506 niche breadth among the megamammal species from Amazon, suggesting a more  
507 generalist diet between C<sub>3</sub>/C<sub>4</sub> resources, tough in C<sub>3</sub> dominant-landscapes. These animals  
508 were native ungulates from Pleistocene of South America with very high-crowned teeth  
509 (hypsodont), presumably used for grazing abrasive plants (Bond et al., 1997). The  
510 isotopic data for *T. platensis*, whose paleoecological interpretations are more complete,  
511 have indicated capacity to feed on a variety of vegetation (Macfadden, 2005). *T. platensis*  
512 possibly had a predominant diet composed by foliage and fruit of wood plants in  
513 southwestern Amazon localities ( $\mu\delta^{13}\text{C} = -13.39 \pm 1.49 \text{ ‰}$ ; median: -13; IQR: -2.35;  
514 Fig. 4C; Macfadden, 2005), different than individuals from the BIR that had a wide food  
515 spectrum, ranging from browsers to grazers on C<sub>3</sub> plants and mixed C<sub>3</sub>-C<sub>4</sub> diets in  
516 woodlands and grasslands, and also in open C<sub>4</sub>-dominated grasslands habitats ( $\mu\delta^{13}\text{C} =$   
517  $-5.08 \pm 5.76 \text{ ‰}$ ; median: -4.22; IQR: -10.81; Fig. 4C; Macfadden, 2005; Viana et al.,  
518 2011; Dantas et al., 2013; França et al., 2014; Dantas et al., 2017; Pansani et al., 2019).  
519 *T. platensis* from Argentinean and Brazilian Pampa also had mixed C<sub>3</sub>/C<sub>4</sub> diets ( $\mu\delta^{13}\text{C} =$   
520  $-6.03 \pm 2.66 \text{ ‰}$ ; median: -5.15; IQR: -3.28; Fig. 4C; Macfadden, 2005; Lopes et al.,

521 2013), whereas the individuals from the Bolivian and Argentinean Chaco had a more  
522 specialized grazer diet in C<sub>4</sub>-dominated open grasslands ( $\mu\delta^{13}\text{C} = 0.38 \pm 1.21 \text{ ‰}$ ; median:  
523  $-0.40$ ; IQR:  $-2$ ; Fig. 4C; Macfadden, 2005).

524 Unfortunately, there are no other paleoecological inferences for *T. lopesi* that would  
525 facilitate the understanding of its feeding behavior. This species had an intertropical  
526 distribution in northern, northeastern and southeastern Brazil and could have coexisted  
527 with *T. platensis*, who was widely distributed in South America (Mendonça, 2012). The  
528 less negative value of carbon isotope from *T. lopesi* suggests a more generalist diet  
529 compared to *T. platensis*. However, this only result is insufficient to presuppose  
530 distinction between their ecological niches, thus more investigations are needed.

531 Regarding large and medium-sized species, the extinct capybara *Nechoerus* sp.  
532 has the highest ecological niche breadth. It presented carbon and oxygen isotope values  
533 very similar to the sympatric *T. lopesi* from Rondônia region (Table 1), indicating a more  
534 C<sub>3</sub>-C<sub>4</sub> generalist diet in wooded savanna habitats closely of <sup>18</sup>O-depleted water sources  
535 (Fig. 3C). The current capybara *Hydrochoerus hydrochaeris* Linnaeus, 1766 has  
536 semiaquatic habit and are native to wetlands in South America. This rodent are folivores  
537 and consumes protein-rich plants near water bodies, particularly grasses and sedges  
538 (Corriale and Loponte, 2015). The carbon stable isotopes from dental bioapatite of  
539 specimens from Amazonian Peru indicate a C<sub>4</sub> diet ( $\mu\delta^{13}\text{C} = -1.6 \pm 3.4\text{ ‰}$ ; Tejada-Lara et  
540 al., 2020), whereas the species in Corrientes province, Argentina, consume predominantly  
541 C<sub>3</sub> grasses and sedges ( $\mu\delta^{13}\text{C}_{\text{collagen}} = -15.7 \pm 0.3 \text{ ‰}$ ;  $\delta^{13}\text{C}_{\text{bioapatite}} = \sim -6 \text{ ‰}$ ; Corriale  
and Loponte, 2015). Thus, based on feeding behavior of living capybaras we presumed  
543 that a significant portion of the Pleistocene capybara diet was also composed of  
544 herbaceous plants.

545 The camelid *P. major* probably had a more selective browser diet ~~for the~~  
546 ~~consumption~~ of dicot foliage plants, due to the very negative  $\delta^{13}\text{C}$  values. Leaves are more  
547 depleted in  $^{13}\text{C}$  than other vegetative structures such as roots, stems and fruits (Badeck  
548 et al., 2005). In addition, this specimen presented  $\delta^{18}\text{O}$  value more positive than other  
549 taxa that could be associated to ingestion of more  $^{18}\text{O}$ -enriched water sources, but could  
550 also be the reflection of a folivore diet, since leaf water is more  $^{18}\text{O}$ -enriched than  
551 meteoric water (Sponheimer and Lee-Torp, 1999). The oxygen isotope aridity index for  
552 several Pleistocene taxa from southeastern and southwestern United States developed by  
553 Yann et al. (2013), discriminates the camelids (i.e., *Palaeolama* and *Hemiauchenia*) with  
554 the greatest mean aridity index followed by antilocaprids and cervids. This supports the  
555 argument that most  $\delta^{18}\text{O}$  values of those taxa comes from the water in food ingested  
556 instead the meteoric water, thus corroborating with the folivore diet inference for the  
557 camelid from southwestern Amazon.

558 The identification of leaves and branches of shrub angiosperms fossil remains in *P.*  
559 *major* coprolites from BIR in Bahia state strengthens the inference of a browser diet  
560 (Marcolino et al., 2012). Stable isotope data from that region indicates significant  
561 consumption of  $\text{C}_3$  plants ( $\delta^{13}\text{C} = - 7.34 \text{ ‰}$ ; Dantas et al., 2020), therefore in a  
562 predominantly open landscape the species probably could inhabit forest edges (Marcolino  
563 et al., 2012). Accordingly, browser habits could be a predominant behavior for this  
564 camelid.

565 For the fossils of extant taxa, *Tapirus* sp. and *Mazama* sp., the fruit consumption  
566 could be more abundant than for the *P. major* in late Pleistocene. The lowland tapir  
567 *Tapirus terrestris* is the largest terrestrial mammal in South America, which occurs from  
568 Colombia to northern Argentina in a wide range of ecosystems, including tropical moist  
569 forest, xeric Chaco and Cerrado forest, savanna wetlands, and lower montane forest

570 (Bodmer, 1990b). *T. terrestris* has a primarily browsing diet, and when the fruits are  
571 available may consume extensively (Bodmer, 1990b). Thus, the tapir plays a key role in  
572 dispersing seeds, especially large ones, for over longer distances, due to their large home  
573 range, varying from 220 to 470 ha (Fragoso et al., 2000, 2003). Similar to our results, the  
574 isotopic data of carbon of extant *T. terrestris* in localities of Brazil, Colombia, Venezuela,  
575 Peru and Bolivia shows low values associated with high proportion of wood plants  
576 consumption ( $\mu\delta^{13}\text{C} = -13.6 \pm 1.6 \text{‰}$ ; DeSantis, 2011).

577 The red brocket deer *Mazama americana* is one of the most abundant and widely  
578 distributed cervids in Neotropical forests (Redford and Eisenberg, 1992; Eisenberg and  
579 Redford, 1999). Its distribution area ranges from Colombia and Venezuela to northern  
580 Argentina and southern Brazil, and also occur in a variety of ecosystems such as montane  
581 forests, lowland dry forest, rainforests and savannas located near forest edges (Emmons  
582 and Feer, 1997). Feeding ecology data from Amazonian populations indicate a fruit and  
583 seed-eating diet, whereas leaves, flowers and fungi are also consumed in less quantity  
584 (Branan et al., 1985; Bodmer, 1990a, Gayot et al., 2004). A seasonal change in feeding  
585 habits was observed by Branan et al. (1985) in Surinam forests, where diet became  
586 folivorous due to fruit scarcity during dry season. Geographic differences in the diet can  
587 be observed comparing studies made in French Guyana (Gayot et al., 2004) and in the  
588 Peruvian Amazon (Bodmer, 1990a), where the proportions of fruit in diet were 56 % and  
589 81 %, respectively.

590 In the Parque Estadual Chandless (PEC), Acre state, *T. terrestris* and *M. americana*  
591 co-occur in a mosaic of heterogeneous forest landscapes, where flood pulses and the  
592 presence of open forests subject to the dynamics exerted by the presence of bamboo form  
593 a complex of successional gradients (Borges, 2014). *T. terrestris* occurs predominantly  
594 in patches of forests near rivers or forest creeks (igarapés) with a predominance of small



595 branches of pioneer plant species and succulent shoots, sometimes it was observed  
596 consuming stems and leaves of young individuals of *Cecropia* sp. and other pioneer  
597 species. *M. americana*, in turn, apparently avoided denser forests and opted for more open  
598 areas. Bodmer (1990) working with large ungulates in the Ucayaly River region, Peru,  
599 found that *M. americana* tends to avoid floodplains, although this pattern was not clearly  
600 noted in the PEC (Borges, 2014).

601 The carbon isotope composition of modern *T. terrestris* and *M. americana* from  
602 Madre de Dios in Peruvian Amazon ( $\mu\delta^{13}\text{C} = -14.6\text{‰} \pm 0.6\text{‰}$  and  $-13.1 \pm 1.1\text{‰}$ ,  
603 respectively; Tejada-Lara et al., 2020), and the carbon isotope composition in collagen  
604 from Venezuelan Amazon ( $\delta^{13}\text{C}_{\text{collagen}} = -23.5\text{‰}$ ;  $\delta^{13}\text{C}_{\text{bioapatite}} = -15.5\text{‰}$  and  $-21.7\text{‰}$ ;  
605  $-14.7\text{‰}$ , respectively; van der Merwe and Medina, 1991) did not diagnose very  
606 significant differences, although the slight difference was attributed to different dietary  
607 compositions between leaves and fruits. These values are similar to our data for the late  
608 Pleistocene, *T. terrestris* ( $\mu\delta^{13}\text{C} = -16.05\text{‰}$ ) with more negative values associated with  
609 a greater preference for more enclosed environments than *Mazama* sp. ( $\delta^{13}\text{C} = -15.47$   
610  $\text{‰}$ ). Thus, we infer that with similar strategies to the present, these ungulates would have  
611 different foraging strategies, varying spatially and even seasonally in order to avoid  
612 interspecific competitions.

613 Finally, the isotope value of carbon suggests a browsing diet for the pampatheriid  
614 *H. rondoniensis* that inhabited mesic woodlands habitats in the Rondônia region, and  
615 contrasts with the dominant grazing habit for the genus suggested by morphological  
616 analysis of teeth and mandibular apparatus (Vizcaíno et al., 1998). Despite the efficiency  
617 in consuming more abrasive vegetation, the previous inference supports that the taxon  
618 was not a strictly grazer. A mixed C<sub>3</sub>-C<sub>4</sub> diet of woody and grassy plants was suggested  
619 by stable isotope analysis for *H. paulacoutoi* species that inhabited the BIR during the

620 late Pleistocene ( $\delta^{13}\text{C} = -6.05\text{‰}$ ; Dantas et al., 2020), indicating that these cingulates  
621 could also have a more generalist diet. *Holmesina* is associated with wetter and warmer  
622 climate environments when compared to the pampatheriid *Pampatherium* from arid and  
623 cold environments (Vizcaíno et al., 1998; De Iuliis et al., 2001; Scillato-Yané et al., 2005),  
624 and may correspond with the occurrence in more forested landscapes in southwestern  
625 Amazonia. It is possible that the analyzed individual of *H. rondoniensis* was foraging on  
626 the understory vegetation, feeding predominantly on foliage and fruits of tree/shrub  
627 plants, although herbaceous plants were also potentially consumed by these animals.

628

629 *4.2.4.4. Niche partitioning strategies and ecological roles from the late*  
630 *Pleistocene mammal assemblages*

631 In terrestrial ecosystems composed by assemblages of large mammals, the  
632 megaherbivores ( $\geq 1,000$  kg) are considered ecological engineers capable of altering  
633 vegetation on a landscape scale. With large body size they may disrupt ecosystem  
634 structure by directly destroying woody vegetation and consuming large amounts of  
635 foliage, and therefore they are generally considered to be limited from the “bottom-up”  
636 by food availability, though exert strong “top-down” control on vegetation structure and  
637 composition (Owen-Smith, 1992).

638 The modern elephant *Loxodonta africana* Blumenbach, 1797 is considered a key  
639 species structuring savanna ecosystems. It acts in the modeling of the environment,  
640 facilitating the access to resources by other middle-sized species, and limiting the  
641 abundance of other megamammal species through the competition for resources (Fritz et  
642 al., 2002).

643 With an ecological role similar to extant elephants, we presuppose that the species  
644 with the largest body mass, *N. platensis* (6,300 kg) and *E. laurillardii* (3,500 kg), were

645 probably the key species that ~~which~~ structured mammal assemblages in the southwestern  
646 Amazon during the late Pleistocene. Both species were potentially competitors, although  
647 the great plasticity and foraging ability of the proboscideans could contribute for a larger  
648 home range and possibility to access different resources. The toxodonts *T. lopesi* and *T.*  
649 *platensis* with a lower similar body mass (~ 1,900 kg) could be competitively excluded,  
650 thus forced to forage slightly more open environments including the woodlands and  
651 arboreal savannas, resulting in a more generalized diet.

652 Species with larger body mass have a more homogeneous spatial distribution than  
653 smaller ones, because their tolerance for lower quality resource consumption (i.e., fibrous  
654 foods with low protein content) allows them to use more diverse habitats, alleviating  
655 interspecific competition (Owen-Smith, 1992). Thus, the camelid *P. major* (~ 280 kg)  
656 that inhabited subcanopies had a possibly strictly folivorous diet, whereas the tapir  
657 *Tapirus* sp. (~ 250 kg) had a more diverse diet and the fruits were important dietary items,  
658 similar to cervid *Mazama* sp. (~ 40 kg). Although, the tapir possibly foraged more in  
659 denser forests and in areas close to water bodies such as igarapés or in floodplain (várzea)  
660 forest and rivers compared to the cervid. The pampatheriid *H. rondoniensis* (~ 120 kg)  
661 was also a browser in this region, but not restricted and could also feed on herbaceous  
662 from understories, and the giant capybara *Nechoerus* sp. (~ 200 kg) with similar diet  
663 behavior as the living *Hydrochoerus*, probably fed predominantly C<sub>3</sub> herbaceous and few  
664 C<sub>4</sub> grasses near water bodies.

665 Comparison of our data with several previous studies about the paleoecology of the  
666 analyzed specimens, permit to assume that resource partitioning and different behaviors  
667 in habitat use were the main mechanisms for reducing interspecific competition and the  
668 maintenance of the coexistence of large herbivorous mammal assemblages that inhabited  
669 the late Pleistocene of southwestern Amazon. Similarly, Dantas et al. (2017) were also

670 able to infer the structure of the assemblages, the partitioning and overlapping niches of  
671 the Pleistocene megamammals that inhabited the BIR, comparing the results of stable  
672 isotopes of carbon and oxygen with the current mammal assemblages of the Africa.

673 The megamammal species probably could have played important roles in the Amazon  
674 forest ecosystem during the late Quaternary, contributing for a greater habitat  
675 heterogeneity (i), because the herbivore pressure may vary across the space, resulting in  
676 a mosaic landscape (Malhi et al., 2016). Greater variation in floristic composition (ii), due  
677 to the large capacity of large fruit seed dispersal for greater distances than large modern  
678 ones as the tapirs, thus contributing to increased gene flow between plant populations  
679 (Guimarães et al., 2008). The megamammals could also contributes increasing the  
680 longevity of mature forest trees and higher forest biomass (iii), due to high pressure by  
681 consumption of the understory and subcanopies plants, which can reduce the below-  
682 ground competition for nutrients (Terborgh et al., 2015a, b), as well as by accelerating  
683 the ecosystem biogeochemical cycling (iv), because nutrients that would be locked for  
684 years in leaves and stems are liberated for use through animal consumption, digestion,  
685 defecation, and urination, and the nutrients in recalcitrant woody biomass are moved to  
686 the decomposition pool through breakage and plant mortality (Malhi et al., 2016).

687

## 688 **5. Conclusions**

689 The carbon ( $\delta^{13}\text{C}$ ) and oxygen ( $\delta^{18}\text{O}$ ) stable isotope analyses aided in the  
690 comprehension of some aspects of feeding ecology and habitats of medium- and mega-  
691 herbivores mammals that inhabited the southwestern Amazon during the late Quaternary.  
692 The isotopic data together with previous paleoecological interpretations of the studied  
693 species, and some information regarding feeding behavior of living species allowed  
694 refining the interpretations about the diet and possible ecological interactions. According

695 to the  $\delta^{13}\text{C}_{\text{VPDB}}$  ( $-17.47\text{‰}$  to  $-8.83\text{‰}$ ) and  $\delta^{18}\text{O}_{\text{VSMOW}}$  ( $19.90$  to  $25.80\text{‰}$ ) results, the 696  
Amazonian late Quaternary mammals inhabited heterogeneous forest habitats, which  
697 facilitated the resource partitioning and the use of distinct habitats. The mammal  
698 assemblages were composed mostly by browsers, with the only exception being the  $\text{C}_3$   
699 and  $\text{C}_4$  generalists *Trigodonops lopesi* and *Nechoerus* sp. ( $p_i\text{C}_3 = \sim 70\%$ ;  $B_A = \sim 0.75$ ).  
700 The largest bodied species, *Eremotherium laurillardi* and *Notiomastodon platensis*, were  
701 probably key species that structured the assemblages through ecosystem modelling,  
702 facilitating the access to resources by other large and middle-sized species (e.g.,  
703 cingulates, tapirs, camelids and cervids), and limiting the abundance of other  
704 megamammal species through the competition for resources (e.g., toxodonts). Further  
705 paleoecological reconstructions are needed, in order to better understand the  
706 paleoenvironmental scenarios and ecological interactions of the mammal species that  
707 inhabited the southwestern Amazon during the late Quaternary.

708

## 709 **Acknowledgments**

710 The authors are grateful to the grant by Academy of Finland for the Subamazon  
711 project, University of Turku, Finland (process number 296406) and the Universidade  
712 Federal do Acre, Rio Branco, Brazil for supporting travelling costs to access the fossil  
713 collections. J. C. Rabelo (Universidade Federal de Mato Grosso) for supporting the  
714 construction of fossiliferous localities map in Arcgis software. Coordenação de  
715 Aperfeiçoamento de Pessoal de Nível Superior (CAPES) for the doctoral scholarship  
716 granted to L. Asevedo (process number 88882.443670/2019-01). Conselho Nacional de  
717 Desenvolvimento Científico e Tecnológico (CNPq) for the financial support through  
718 Universal project (process number 404684/2016-5) and research fellowship for M.A.T.  
719 Dantas (PQ/CNPq 311003/2019-2). The authors are also thankful to the

720 anonymous reviewers for their valuable comments and suggestions for improving the  
721 quality of this paper.

722

## 723 **6. References**

724 Alberdi, M.T., Cerdeño, E., Prado, J.L., 2008. *Stegomastodon platensis*(Proboscidea,  
725 Gomphotheriidae) en el Pleistoceno de Santiago del Estero, Argentina. *Ameghiniana*.  
726 45(2), 257-271.

727 Anderson, J. F., Hall- Martin, A., Russell, D. A., 1985. Long- bone circumference and  
728 weight in mammals, birds and dinosaurs. *Journal of Zoology*. 207(1), 53-61.

729 Arruda, D. M., Schaefer, C. E., Fonseca, R. S., Solar, R. R., Fernandes- Filho, E. I., 2018.  
730 Vegetation cover of Brazil in the last 21 ka: New insights into the Amazonian refugia  
731 and Pleistocenic arc hypotheses. *Global Ecology and Biogeography*. 27(1), 47-56.

732 Asevedo, L., Winck, G. R., Mothé, D., Avilla, L. S., 2012. Ancient diet of the Pleistocene  
733 gomphothere *Notiomastodon platensis* (Mammalia, Proboscidea, Gomphotheriidae)  
734 from lowland mid-latitudes of South America: Stereomicrowear and tooth calculus  
735 analyses combined. *Quaternary International*.255, 42-52.

736 Asevedo, L., D'Apolito, C., Misumi, S. Y., Barros, M. A., Barth, O. M., Avilla, L. S.,  
737 2020. Palynological analysis of dental calculus from Pleistocene proboscideans of  
738 southern Brazil: A new approach for paleodiet and paleoenvironmental  
739 reconstructions. *Palaeogeography, Palaeoclimatology, Palaeoecology*. 540, 109523.

740 Ayliffe, L.K., Lister, A.M., Chivas, A.R., 1992. The preservation of glacial-interglacial  
741 climatic signatures in the oxygen isotopes of elephant skeletal phosphate.  
742 *Palaeogeography, Palaeoclimatology, Palaeoecology*. 99, 179-191.

743 Badeck, F. W., Tcherkez, G., Nogues, S., Piel, C., Ghashghaie, J., 2005. Post-  
744 photosynthetic fractionation of stable carbon isotopes between plant organs—a

745 widespread phenomenon. *Rapid Communications in Mass Spectrometry: An*  
746 *International Journal Devoted to the Rapid Dissemination of Up- to- the- Minute*  
747 *Research in Mass Spectrometry.* 19 (11), 1381-1391.

748 Bargo, M. S., Toledo, N., Vizcaíno, S. F., 2006. Muzzle of South American Pleistocene  
749 ground sloths (*Xenarthra*, Tardigrada). *Journal of Morphology.* 267(2), 248-263.

750 Bodmer, R. E., 1990a. Responses of ungulates to seasonal inundations in the Amazon  
751 floodplain. *Journal of tropical Ecology.* 6 (2), 191–201.

752 Bodmer, R. E., 1990b. Fruit patch size and frugivory in the lowland tapir (*Tapirus*  
753 *terrestris*). *Journal of Zoology.* 222 (1), 121–128.

754 Bond, M., Cerdeño, E., López, G., 1997. Los ungulados nativos de América del Sur. In:  
755 Alberdi, M.T., Leone, G., Tonni, E.P. (Eds.), *Evolución Biológica y Climática de la*  
756 *Region Pamapeana durante los Últimos Cinco Millones de Años. Monografías*  
757 *Museo Nacional de Ciencias Naturales, Madrid, pp. 257–275.*

758 Borges, L. H. M., 2014. Abundância de mamíferos de médio e grande porte em resposta  
759 ao grau de distanciamento do rio Chandless, Parque Estadual Chandless, Acre,  
760 Brasil. Universidade Federal do Acre, Rio Branco, M.Sc. thesis, 69p.

761 Branan, W. V., Werkhoven, M. C., Marchinton, R. L., 1985. Food habits of brocket and  
762 white-tailed deer in Suriname. *The Journal of wildlife management.* 49, 972-976.

763 Bryant, J.D., Koch, P.L., Froelich, P.N., Showers, W.J., Genna, B.J., 1996. Oxygen  
764 isotope partitioning between phosphate and carbonate in mammalian apatite.  
765 *Geochimica et Cosmochimica Acta.* 60(24), 5145-5148.

766 Bush, M.B., Weimann, M., Piperno, D.R., Liu, K.K.B., Colinvaux, P.A., 1990.  
767 Pleistocene temperature depression and vegetation change in Ecuadorian Amazonia.  
768 *Quaternary Research.* 34, 330–45.

769 Bush, M.B., Oliveira, P.E., Colinvaux, P.A., Miller, M.C., Moreno, J.E., 2004.  
770 Amazonian palaeoecological histories: One Hill, Three Watersheds.  
771 Palaeogeography, Palaeoclimatology, Palaeoecology. 214, 359–93.

772 Cerling, T. E., Harris, J. M., 1999. Carbon isotope fractionation between diet and  
773 bioapatite in ungulate mammals and implications for ecological and paleoecological  
774 studies. *Oecologia*. 120(3), 347-363.

775 Cheng, H., Sinha, A., Cruz, F.W., Wang, X., Edwards, R.L., d'Horta, F.M., Ribas, C.C.,  
776 Vuille, M., Stott, L.D., Auler, A.S., 2013. Climate change patterns in Amazonia  
777 and biodiversity. *Nature communications*. 4(1), 1-6.

778 Cherkinsky, A., 2009. Can we get a good radiocarbon age from “bad bone”? Determining  
779 the reliability of radiocarbon age from bioapatite. *Radiocarbon*. 51-2, 647-655.

780 Cohen, M. C. L., Rossetti, D. F., Pessenda, L. C. R., Friaes, Y. S., Oliveira, P. E., 2014.  
781 Late Pleistocene glacial forest of Humaitá-Western Amazonia. *Palaeogeography,*  
782 *Palaeoclimatology, Palaeoecology*. 415, 37-47.

783 Colinvaux, P.A., Oliveira, P.E., Moreno, J.E., Miller, M.C., Bush, M.B., 1996. A long  
784 pollen record from lowland Amazonia: forest and cooling in glacial times. *Science*.  
785 274, 85–8.

786 Colinvaux, P.A., Oliveira, P.E., Bush, M.B., 2000. Amazonian and neotropical plant  
787 communities on glacial time-scales: the failure of the aridity and refuge hypotheses.  
788 *Quaternary Science Reviews*. 19, 141–69.

789 Colinvaux, P.A., Irion, G., Räsänen, M.E., Bush, M.B., Mello, J.A.S.N., 2001. A paradigm  
790 to be discarded: geological and paleoecological data falsify the Haffer and Prance  
791 refuge hypothesis of Amazonian speciation. *Amazoniana*. 16, 609–46.

792 Coplen, T. B., 1994. Reporting of stable hydrogen, carbon, and oxygen isotopic  
793 abundances (technical report). *Pure and Applied Chemistry*. 66(2), 273-276.



794 Corriale, M. J., Loponte, D., 2015. Use of stable carbon isotope ratio for foraging behavior  
795 analysis of capybara (*Hydrochoerus hydrochaeris*) from Esteros del Iberá,  
796 Argentina. *Mammalian Biology*. 80(2), 73-80.

797 Dantas, M. A. T., Xavier, M. C. T., França, L.M., Cozzuol, M. A., Ribeiro, A.S.,  
798 Figueiredo, A. M. G., Kinoshita, A., Baffa, O., 2013. A review of the time scale and  
799 potential geographic distribution of *Notiomastodon platensis* (Ameghino, 1888) in  
800 the late Pleistocene of South America. *Quaternary International*. 317, 73-79.

801 Dantas, M. A. T., Cherkinsky, A., Bocherens, H., Drefahl, M., Bernardes, C., França, L.  
802 M., 2017. Isotopic paleoecology of the Pleistocene megamammals from the Brazilian  
803 Intertropical Region: Feeding ecology ( $\delta^{13}\text{C}$ ), niche breadth and overlap. *Quaternary*  
804 *Science Reviews*. 170, 152-163.

805 Dantas, M. A. T., 2019. Atualizando a estimativa da massa corporal da megafauna do  
806 Pleistoceno Final da Região Intertropical Brasileira. In: XXVI Congresso Brasileira  
807 de Paleontologia, Uberlândia, Minas Gerais, Brazil. *Paleontologia em Destaque*,  
808 219-220p.

809 Dantas, M. A. T., Cherkinsky, A., Lessa, C. M. B., Santos, L.V., Cozzuol, M.A., Omena,  
810 E.C., Silva, J.L.L., Sial, A.N., Bocherens, H., 2020. Isotopic Paleoecology ( $\delta^{13}\text{C}$ ,  
811  $\delta^{18}\text{O}$ ) of Late Quaternary megafauna from Brazilian Intertropical Region. *Revista*  
812 *Brasileira de Paleontologia*, v. 23, n 2.

813 De Iuliis, G., Bargo, M. S., Vizcaíno, S. F., 2001. Variation in skull morphology and  
814 mastication in the fossil giant armadillos *Pampatherium* spp. and allied genera  
815 (Mammalia: Xenarthra: Pampatheriidae), with comments on their systematics and  
816 distribution. *Journal of Vertebrate Paleontology*. 20(4), 743-754.

817 Domingo, L., Prado, J.L., Alberdi, M.T., 2012. The effect of paleoecology and  
818 paleobiogeography on stable isotopes of Quaternary mammals from South America.  
819 Quaternary Sciences Review. 55, 103-113.

820 Duarte, J. M. B., Jorge, W., 1996. Chromosomal polymorphism in several populations of  
821 deer (genus *Mazama*) from Brazil. *Archivos de Zootecnia*. 45, 281-287.

822 Ehleringer, J.R., Cerling, T.E., 2002. C3 and C4 photosynthesis. In: Mooney, H.A.,  
823 Canadell, J.G. (Eds.), *The earth system: biological and ecological dimensions of*  
824 *global environmental change*. Chichester: John Wiley & Sons, Ltd, v. 2, p. 186–90.

825 Eisenberg, J.F., Redford, K.M., 1999. *Mammals of the Neotropics: The central*  
826 *Neotropics*. Chicago, University of Chicago Press.

827 Emmons, L.H., Feer, F., 1997. *Neotropical rainforest mammals: A field guide*. 2 ed.  
828 Chicago: The University of Chicago Press.

829 Fortelius, M., Solounias, N., 2000. Functional characterization of ungulate molars using  
830 the abrasion-attrition wear gradient: a new method for reconstructing  
831 paleodiets. *American Museum Novitates*. 2000(3301), 1-36.

832 Fragoso, J. M., Huffman, J. M., 2000. Seed-dispersal and seedling recruitment patterns  
833 by the last Neotropical megafaunal element in Amazonia, the tapir. *Journal of*  
834 *Tropical Ecology*. 16(3), 369-385.

835 Fragoso, J. M., Silvius, K. M., Correa, J. A., 2003. Long- distance seed dispersal by tapirs  
836 increases seed survival and aggregates tropical trees. *Ecology*. 84(8), 1998-2006.

837 França, L. M., Dantas, M. A. T., Bocchiglieri, A., Cherckinsky, A., Ribeiro, A. S.,  
838 Bocherens, H., 2014. Chronology and ancient feeding ecology of two upper  
839 Pleistocene megamammals from the Brazilian Intertropical Region. *Quaternary*  
840 *Science Reviews*. 99, 78-83.

- 841 Freitas, H. A., Pessenda, L. C. R., Aravena, R., Gouveia, S. E. M., Ribeiro, A. S., Boulet,  
842 R., 2001. Late Quaternary vegetation dynamics in the southern Amazon basin  
843 inferred from carbon isotopes in soil organic matter. *Quaternary Research*. 55(1), 39-  
844 46.
- 845 Fricke, H., 2007. Stable Isotope Geochemistry of Bonebed Fossils: Reconstructing  
846 Paleoenvironments, Paleoecology, and Paleobiology. In: Rogers, R.R., Eberth, D.A.,  
847 Fiorillo, A.R. (Eds.). *Bonebeds: Genesis, Analysis, and Paleobiological Significance*.  
848 The University of Chicago Press, p. 437-490.
- 849 Fritz, H., Duncan, P., Gordon, I.J., Illius, A.W., 2002. Megaherbivores influence trophic  
850 guilds structure in African ungulate communities. *Oecologia*. 131, 620-625.
- 851 Gayot, M., Henry, O., Dubost, G., Sabatier, D., 2004. Comparative diet of the two forest  
852 cervids of the genus *Mazama* in French Guiana. *Journal of Tropical Ecology*. 20(1),  
853 31-43.
- 854 Ghizzoni, M., 2014. Estimación de lamasa corporal de  
855 un ejemplar cuaternario del carpincho extinto *Neochoerus* a través de medidas cráneo-  
856 dentales. *Revista Brasileira Paleontologia*. 17, 83-90.
- 857 Góis, F., Nascimento, E. D., Porto, A. S., Holanda, E. C., Cozzuol, M. A., 2004.  
858 Ocorrências de Cingulata dos gêneros *Kraglievichia* e *Holmesina* do Terciário e  
859 Quaternário da Amazônia Sul-Occidental. *Ameghiniana*. 41(4), 49R.
- 860 Guimarães Jr, P. R., Galetti, M., Jordano, P., 2008. Seed dispersal anachronisms:  
861 rethinking the fruits extinct megafauna ate. *PloSone*, 3(3), e1745.
- 862 Gutiérrez, M., Alberdi, M. T., Prado, J. L., Perea, D., 2005. Late Pleistocene  
863 *Stegomastodon* (Mammalia, Proboscidea) from Uruguay. *Neues Jahrbuch für*  
864 *Geologie und Palaontologie-Monatshefte*. 11, 641-662.
- 865 Haffer, J., 1969. Speciation in Amazonian forest birds. *Science* 165, 131-7.

866 Higgins, P., 2018. Isotope ecology from biominerals. In: D. A. Croft, D. F. Su, S. W.  
867 Simpson (Eds.), *Methods in paleoecology: Reconstructing Cenozoic terrestrial*  
868 *environments and ecological communities*. Springer, p. 99–120.

869 Holanda, E. C., Cozzuol, M. A., 2006. New records of *Tapirus* from the late Pleistocene  
870 of southwestern Amazonia, Brazil. *Revista Brasileira de Paleontologia*. 9(2), 193-  
871 200.

872 Holanda, E. C., Ferigolo, J., Ribeiro, A. M., 2011. New *Tapirus* species (Mammalia:  
873 Perissodactyla: Tapiridae) from the upper Pleistocene of Amazonia,  
874 Brazil. *Journal of Mammalogy*. 92(1), 111-120.

875 IBGE. *Manual Técnico da Vegetação Brasileira*. Rio de Janeiro, 2012.

876 Irion, G., Bush, M.B., Mello, J.A.N., Stüben, D., Neumann, T., Müller, R.G., Moraes,  
877 J.O., Junk, J.W., 2006. A multiproxy palaeoecological record of Holocene lake  
878 sediments from the Rio Tapajós, eastern Amazonia. *Palaeogeography,*  
879 *Palaeoclimatology, Palaeoecology*. 240, 523–36.

880 Keeling, C. D., 1979. The Suess effect: <sup>13</sup>Carbon-<sup>14</sup>Carbon interrelations. *Environment*  
881 *International*. 2 (4-6), 229-300.

882 Koch, P.L., 2007. Isotopic study of the biology of modern and fossil vertebrates. In:  
883 Michener, R., Lajtha, K. (eds.). *Stable Isotopes in Ecology and Environmental*  
884 *Science*. 2a edição. Blackwell Publishing, p. 99-154.

885 Kohn, M. J., 2010. Carbon isotope compositions of terrestrial C3 plants as indicators of  
886 (paleo) ecology and (paleo) climate. *Proceedings of the National Academy of*  
887 *Sciences*. 107(46), 19691-19695.

888 Latrubesse, E. M., Rancy, A., 1998. The late Quaternary of the Upper Juruá River,  
889 southwestern Amazonia, Brazil: geology and vertebrate paleontology. *Quaternary of*  
890 *South America and Antarctic Peninsula*. 11(2), 27-46.

- 891 Ledru, M.P., 2002. Late Quaternary history and evolution of the cerrados as revealed by  
892 palynological records. In: Oliveira PS, Marquis RJ, editors. The Tropical Cerrados  
893 of Brazil: Ecology and Natural History of a Neotropical Savanna. New  
894 York:University Press. p 33–52.
- 895 Ledru, M. P, Ceccantini, G., Gouveia, S.E.M., López-Sáez, J.A., Pessenda, L.C.R.,  
896 Riberito, A.S., 2006. Millennial-scale climatic and vegetation changes in a northern  
897 Cerrado (Northeast, Brazil) since the Last Glacial Maximum. *Quaternary Science*  
898 *Reviews*. 25,1110–26.
- 899 Levin, N. E., Cerling, T. E., Passey, B. H., Harris, J. M., Ehleringer, J. R., 2006. A stable  
900 isotope aridity index for terrestrial environments. *Proceedings of the National*  
901 *Academy of Sciences*. 103(30), 11201-11205.
- 902 Levins, R., 1968. *Evolution in changing environments: some theoretical*  
903 *explorations*. New Jersey, Princeton University Press, No. 2, 120p.
- 904 Liu, K.B, Colinvaux, P.A., 1985. Forest changes in the Amazon Basin during the last  
905 glacial maximum. *Nature*. 318, 556–7.
- 906 Lopes, R. P., Ribeiro, A. M., Dillenburg, S. R., Schultz, C. L., 2013. Late middle to late  
907 Pleistocene paleoecology and paleoenvironments in the coastal plain of Rio Grande  
908 do Sul State, Southern Brazil, from stable isotopes in fossils of *Toxodon* and  
909 *Stegomastodon*. *Palaeogeography, Palaeoclimatology, Palaeoecology*. 369, 385-394.
- 910 MacFadden, B. J., Higgins, P., 2004. Ancient ecology of 15-million-year-old browsing  
911 mammals within C3 plant communities from Panama. *Oecologia*. 140(1), 169-182.
- 912 MacFadden, B. J., 2005. Diet and habitat of toxodont megaherbivores (Mammalia,  
913 Notoungulata) from the late Quaternary of South and Central America. *Quaternary*  
914 *Research*. 64(2), 113-124.

- 915 Marcolino, C. P., Isaias, R. M. S., Cozzuol, M. A., Cartelle, C., Dantas, M. A. T., 2012.  
916 Diet of *Palaeolama major* (Camelidae) of Bahia, Brazil, inferred from  
917 coprolites. *Quaternary International*. 278, 81-86.
- 918 Marshall, J.D., Brooks, J.R., Lajtha, K., 2007. Sources of variation in the stable isotopic  
919 composition of plants. In: Michener, R., Lajtha, K. (eds.). *Stable Isotopes in Ecology  
920 and Environmental Science*. 2a edição. Blackwell Publishing, p. 22-60.
- 921 Mayle, F.E., Power, M.J., 2008. Impact of a drier Early–Mid-Holocene climate upon  
922 Amazonian forests. *Philosophical Transactions of the Royal Society B*. 363, 1829–38.
- 923 Mendonça, R., 2012. Diversidade de toxodontes pleistocênicos (Notoungulata,  
924 Toxodontidae): uma nova visão. Universidade de São Paulo, Doctoral thesis, 151p.
- 925 Mosblech, N.A.S., Bush, M.B., Gosling, W.D., Hodell, D., Thomas, L., van Calsteren,  
926 P., Correa-Metrio, A., Valencia, B.G., Curtis, J., van Woesik, R., 2012. North  
927 Atlantic forcing of Amazonian precipitation during the last ice age.  
928 *Nature Geoscience*. 5(11), 817-820.
- 929 Mothé, D., Avilla, L. S., Asevedo, L., Borges-Silva, L., Rosas, M., Labarca-Encina, R.,  
930 Souberlich, R., Soibelzon, E., Roman-Carrion, J. L., Ríos, S. D., Rincon, A. D.,  
931 Oliveira, G. C., Lopes, R. P., 2017. Sixty years after ‘The mastodonts of Brazil’: The  
932 state of the art of South American proboscideans (Proboscidea,  
933 Gomphotheriidae). *Quaternary International*. 443, 52-64.
- 934 Naples, V. L., McAfee, R. K., 2012. Reconstruction of the cranial musculature and  
935 masticatory function of the Pleistocene panamerican ground sloth *Eremotherium  
936 laurillardii* (Mammalia, Xenarthra, Megatheriidae). *Historical Biology*. 24(2), 187-  
937 206.
- 938 Nascimento, E. R., 2008. Os Xenarthra Pilosa (Megatheriidae), Notoungulata  
939 (Toxodontidae) e Proboscidea (Gomphotheriidae) da Formação Rio Madeira,

940 Pleistoceno superior, Estado de Rondônia, Brasil. Universidade Federal do Rio  
941 Grande do Sul, M.Sc. thesis, 113p.

942 Nelson, S. V., 2013. Chimpanzee fauna isotopes provide new interpretations of fossil ape  
943 and hominin ecologies. Proceedings of the Royal Society B: Biological  
944 Sciences. 280(1773), 20132324.

945 Oliveira, J. F., Asevedo, L., Cherkinsky, A., Dantas, M. A. T., 2020. Radiocarbon dating  
946 and integrative paleoecology ( $\delta^{13}\text{C}$ , stereomicrowear) of *Eremotherium laurillardi*  
947 (Lund, 1842) from midwest region of the Brazilian intertropical region. Journal of  
948 South American Earth Sciences, 102653.

949 Olivier, J., Otto, T., Roddaz, M., Antoine, P. O., Londoño, X., Clark, L. G., 2009. First  
950 macrofossil evidence of a pre-Holocene thorny bamboo cf. *Guadua* (Poaceae:  
951 Bambusoideae: Bambuseae: Guaduinae) in south-western Amazonia (Madre de  
952 Dios—Peru). Review of Palaeobotany and Palynology. 153(1-2), 1-7.

953 Owen-Smith, N., 1992. Megaherbivores: The influence of very large body size on  
954 Ecology. Cambridge Univ Press, Cambridge, UK.

955 Padilla, M., Dowler, R.C., 1994. *Tapirusterrestris*. Mammalian Species: American  
956 Society of Mammalogists. N 481. Northampton. 1-8 p.

957 Pansani, T. R., Muniz, F. P., Cherkinsky, A., Pacheco, M. L. A. F., Dantas, M. A. T.,  
958 2019. Isotopic paleoecology ( $\delta^{13}\text{C}$ ,  $\delta^{18}\text{O}$ ) of Late Quaternary megafauna from Mato  
959 Grosso do Sul and Bahia States, Brazil. Quaternary Science Reviews. 221,  
960 105864. Parssinen, M., Balee, W., Ranzi, A., Barbosa, A., in press. Evidence of 10  
961 000-year-old human land-use practices, fires and climate in the geoglyph sites of  
962 Southwestern Amazonia. Antiquity.

- 963 Paula Couto, 1982. Fossil mammals from the Cenozoic of Acre, Brasil. V-  
964 Notoungulata Nesodontinae (II), Toxodontidae and Haplodontiinae, and Litopterna,  
965 Pyrotheria and Astrapotheria (II). Iheringia. Série geologia. N 7, P 5
- 966 Paula-Couto, C. D., 1983a. Fossil mammals from the Cenozoic of Acre, Brazil, VI-  
967 Edentata Cingulata. Iheringia, Série Geologia, 8, 33-49.
- 968 Paula Couto, C. P., 1983b. Fossil Mammals from the Cenozoic of Acre Brasil. vii-  
969 Miscellanea. Iheringia Série Geologia Porto Alegre, 8, 101-120.
- 970 Pessenda, L. C. R., Gomes, B. M., Aravena, R. R. A. S., Ribeiro, A. D. S., Boulet, R.,  
971 Gouveia, S. E. M., 1998. The carbon isotope record in soils along a forest-cerrado  
972 ecosystem transect: implications for vegetation changes in the Rondonia state,  
973 southwestern Brazilian Amazon region. *The Holocene*. 8(5), 599-603.
- 974 Phillips, D. L., 2012. Converting isotope values to diet composition: the use of mixing  
975 models. *Journal of Mammalogy*. 93(2), 342-352.
- 976 Pianka, E. R., 1973. The structure of lizard communities. *Annual review of ecology and*  
977 *systematics*. 4(1), 53-74.
- 978 Porto, A. S., Góis, F., Nascimento, E. D., Holanda, E. C., Cozzuol, M. A., 2004. *Xenarthra*  
979 *Pilosa (Edentata) do Quaternário do Estado de Rondônia. Ameghiniana*  
980 *Suplemento*. 41, 60R.
- 981 Ranzi, A., 2000. *Paleoecologia da Amazônia: megafauna do Pleistoceno*. Florianópolis:  
982 EDUFSC, 2000. 101 p.
- 983 Ranzi, A., 2008. *Paleontologia da Amazônia: mamíferos fósseis do Juruá*. Rio Branco:  
984 M.M. Paim Representações e Comércio. 130 p.
- 985 Redford, K.H., Eisenberg, J.F., 1992. *Mammals of the Neotropics: The southern cone*.  
986 Chicago, University of Chicago Press.



987 Reimer, P.J., Bard, E., Bayliss, A., Beck, J.W., Blackwell, P.G., Bronk Ramsey, C., Buck,  
988 C.E., Cheng, H., Edwards, R.L., Friedrich, M., Grootes, P.M., Guilderson, T.P.,  
989 Haflidason, H., Hajdas, I., Hatt\_e, C., Heaton, T.J., Hogg, A.G., Hughen, K.A.,  
990 Kaiser, K.F., Kromer, B., Manning, S.W., Niu, M., Reimer, R.W., Richards, D.A.,  
991 Scott, E.M., Southon, J.R., Turney, C.S.M., Van der Plicht, J., 2013. IntCal13 and  
992 MARINE13 radiocarbon age calibration curves 0-50000 years calBP. Radiocarbon  
993 55 (4), 1869e1887

994 Rizzotto, G. J., De Oliveira, J.G.F., 2005. Projeto Rio Madeira - levantamento de  
995 informações para subsidiar o estudo de viabilidade do aproveitamento hidroelétrico  
996 (AHE) do Rio Madeira. Relatório Final. CPRM–Serviço Geológico do Brasil, Porto  
997 Velho, Brazil.

998 Rossetti, D. F., Cohen, M. C., Pessenda, L. C., 2017. Vegetation change in Southwestern  
999 Amazonia (Brazil) and relationship to the late Pleistocene and Holocene  
1000 climate. Radiocarbon, 59 (1), 69-89.

1001 Sánchez, B., Prado, J. L., Alberdi, M. T., 2004. Feeding Ecology, dispersal, and extinction  
1002 of South American Pleistocene gomphotheres (Gomphotheriidae, Proboscidea).  
1003 Paleobiology. 30 (1), 146-161.

1004 Scillato-Yané, G. J., Carlini, A. A., Tonni, E. P., Noriega, J. I., 2005. Paleobiogeography  
1005 of the late Pleistocene pampatheres of South America. Journal of South American  
1006 Earth Sciences. 20(1-2), 131-138.

1007 Simpson, G.G., Paula Couto, C., 1981. Fossil mammals from the Cenozoic of Acre, Brazil  
1008 III - Pleistocene Edentata Pilosa, Proboscidea, Sirenia, Perissodactyla and  
1009 Artiodactyla. Iheringia. Série geologia. N 6, P 11-73.

1010 Solounias, N., Semprebon, G., 2002. Advances in the reconstruction of ungulate  
1011 ecomorphology with application to early fossil equids. *American*  
1012 *Museum Novitates*. 2002(3366), 1-49.

1013 Sponheimer, M., Lee-Thorp, J. A., 1999. Oxygen isotopes in enamel carbonate and their  
1014 ecological significance. *Journal of Archaeological Science*. 26(6), 723-728.

1015 Tejada-Lara, J. V., MacFadden, B. J., Bermudez, L., Rojas, G., Salas-Gismondi, R.,  
1016 Flynn, J. J., 2018. Body mass predicts isotope enrichment in herbivorous  
1017 mammals. *Proceedings of the Royal Society B: Biological Sciences*. 285(1881),  
1018 20181020.

1019 Tejada, J. V., Flynn, J. J., Antoine, P. O., Pacheco, V., Salas-Gismondi, R., Cerling, T.  
1020 E., 2020. Comparative isotope ecology of western Amazonian rainforest  
1021 mammals. *Proceedings of the National Academy of Sciences*. 117(42), 26263-  
1022 26272.

1023 Terborgh, J., Davenport, L.C., 2015a. Megafaunal influences on tree recruitment in  
1024 African equatorial forests. *Ecography (Cop)*, 10.1111/ecog.01641.

1025 Terborgh J., et al., 2015b. The African rainforest: Odd man out or megafaunal landscape?  
1026 African and Amazonian forests compared. *Ecography*. 39,187-193.

1027 van Breukelen, M. R., Vonhof, H. B., Hellstrom, J. C., Wester, W. C. G., Kroon, D., 2008.  
1028 Fossil dripwater in stalagmites reveals Holocene temperature and rainfall variation  
1029 in Amazonia. *Earth and Planetary Science Letters*. 275, 54–60.

1030 van der Hammen, T., Absy, M.L., 1994. Amazonia during the last glacial.  
1031 *Palaeogeography, Palaeoclimatology, Palaeoecology*. 109, 247–61.

1032 van der Hammen, T., Hooghiemstra, H., 2000. Neogene and Quaternary history  
1033 of vegetation, climate and plant diversity in Amazonia. *Quaternary Science Reviews*.  
1034 19, 725–42.

1035 van der Merwe, N. J., Medina, E., 1991. The canopy effect, carbon isotope ratios and  
1036 foodwebs in Amazonia. *Journal of Archaeological Science*. 18(3), 249-259.

1037 Viana, M.S.S., Silva, J.L.L., Oliveira, P.V., Julião, M.S.S., 2011. Hábitos alimentares em  
1038 herbívoros da megafauna pleistocênica no nordeste do Brasil. *Estudos Geológicos*.  
1039 21 (2), 89–95.

1040 Vizcaíno, S. F., De Iuliis, G., Bargo, M. S., 1998. Skull shape, masticatory apparatus, and  
1041 diet of *Vassallia* and *Holmesina* (Mammalia: Xenarthra: Pamphathiidae): when  
1042 anatomy constrains destiny. *Journal of Mammalian Evolution*. 5(4), 291-322.

1043 Yann, L. T., DeSantis, L. R., Haupt, R. J., Romer, J. L., Corapi, S. E., Ettenson, D. J.,  
1044 2013. The application of an oxygen isotope aridity index to terrestrial  
1045 paleoenvironmental reconstructions in Pleistocene North America.  
1046 *Paleobiology*. 39(4), 576-590.

1047

#### 1048 **Figure captions**

1049 Fig. 1. Localities of the late Quaternary mammals from southwestern Amazon at along  
1050 the banks of Juruá (locality 1, a-d) and Chandless rivers (locality 2) in Acre state, as also  
1051 in Araras locality, Madeira Rriver (locality 3) in Rondônia state, Brazil. The localities  
1052 of *Toxodon platensis* from Peru and Bolivia (localities 4-9) are from Macfadden (2005).

1053

1054 Fig. 2. Bivariate plot with  $\delta^{13}\text{C}_{\text{VPDB}}$  and  $\delta^{18}\text{O}_{\text{VSMOW}}$  values from late Quaternary  
1055 herbivorous mammals of the southwestern Amazonia. The enrichment ranges of  $\delta^{13}\text{C}$   
1056 values were according to the body mass by Tejada-Lara et al. (2018). A) species with  
1057 body mass > 3,500 kg ( $\epsilon^* = 15 \text{ ‰}$ ). B) species with body mass between 3,500 to 600 kg  
1058 ( $\epsilon^* = 14 \text{ ‰}$ ). C) species with body mass between 600 to 75 kg and < 75 kg ( $\epsilon^* = 13$  and

1059 12 ‰, respectively). The traces represent the average of  $\delta^{13}\text{C}$  values for  $\text{C}_3$  and  $\text{C}_4$   
1060 resources.

1061

1062 Fig. 3. Reconstruction of late Quaternary herbivorous mammals from southwestern  
1063 Amazon in distinct phytodomains. A) *Tapirus* sp., *Palaeolama major*, *Notiomastodon*  
1064 *platensis* and *Eremotherium laurillardi* (from left to right) in closed-canopy forest habitat.  
1065 B) *Holmesina rondoniensis*, *Toxodon platensis* and *Mazama* sp. (from left to right) in  
1066 mesic woodland, and C) *Nechoerus* sp. and *Trigodonops lopesi* in arboreal savanna  
1067 habitat. Artist Beatriz Grigio.

1068 Fig. 4. BOX-plot of  $\delta^{13}\text{C}_{\text{VPDB}}$  values for the Pleistocene megaherbivores species  
1069 *Eremotherium laurillardi* (A), *Notiomastodon platensis* (B), *Toxodon platensis* and  
1070 *Trigodonops lopesi* (C) from southwestern Amazon compared to different ecoregions  
1071 from South America. Abbreviation: Tri = *Trigodonops lopesi*. Ecoregions: Brazilian  
1072 Intertropical Region (= BIR; Northeast, Midwest and Southeast of Brazil; Sánchez et al.,  
1073 2004; Macfadden, 2005; Viana et al., 2011; Dantas et al., 2013, França et al., 2014;  
1074 Pansani et al., 2019; Dantas et al., 2017), Andean (Ecuador and Peru; Sánchez et al.,  
1075 2004; Domingo et al., 2012), Chaco (Bolivia and Argentina; Macfadden, 2005; Alberdi et  
1076 al., 2008; Domingo et al., 2012) and Pampa (Argentina, Uruguay and Brazil; Sánchez et  
1077 al., 2004; Macfadden, 2005; Gutiérrez et al., 2005; Domingo et al., 2012; Lopes et al.,  
1078 2013).

1079

#### 1080 **Table caption**

1081 Table 1. Mean values of  $\delta^{13}\text{C}_{\text{VPDB}}$  and  $\delta^{18}\text{O}_{\text{VSMOW}}$ , proportional contributions of diet  
1082 sources ( $pi\text{C}_3$  plants,  $pi\text{C}_4$  plants) and standardized isotopic niche breadth ( $B_A$ ) from  
1083 Quaternary mammal assemblages of southwestern Amazon. A) Araras, Madeira River,

1084 Rondônia state, B) Upper Juruá and Chandless rivers, Acre state, Brazil, C) and D)  
1085 localities of Bolivia and Peru, respectively from Macfadden (2005). Acronym: BM =  
1086 Body mass. References: a: Dantas et al. (2020), b: Dantas (2019), c: Padilla and Dowler  
1087 (1994), d: Ghizzoni (2014), e: Duarte and Jorge (1996).

1088

1089 Table 2. Values of  $\delta^{18}\text{O}_{\text{P-VSMOW}}$  and  $\delta^{18}\text{O}_{\text{mwVSMOW}}$  obtained from oxygen isotopes in  
1090 carbonate enamel ( $\delta^{18}\text{O}_{\text{C}}$ ) of *Notiomastodon platensis* from southwestern Amazon.

1091

### 1092 **Supplementary material**

1093 Supplementary Table 1. Summary data of  $\delta^{13}\text{C}_{\text{VPDB}}$  and  $\delta^{18}\text{O}_{\text{VSMOW}}$  values and  $^{14}\text{C}$  AMS  
1094 datings of Quaternary mammal species from southwestern Amazon. Abbreviations: E =  
1095 enamel, D = dentine and B = bone. Carbon and oxygen isotope data of *Toxodon platensis*  
1096 from Peru and Bolivia by Macfadden (2005).

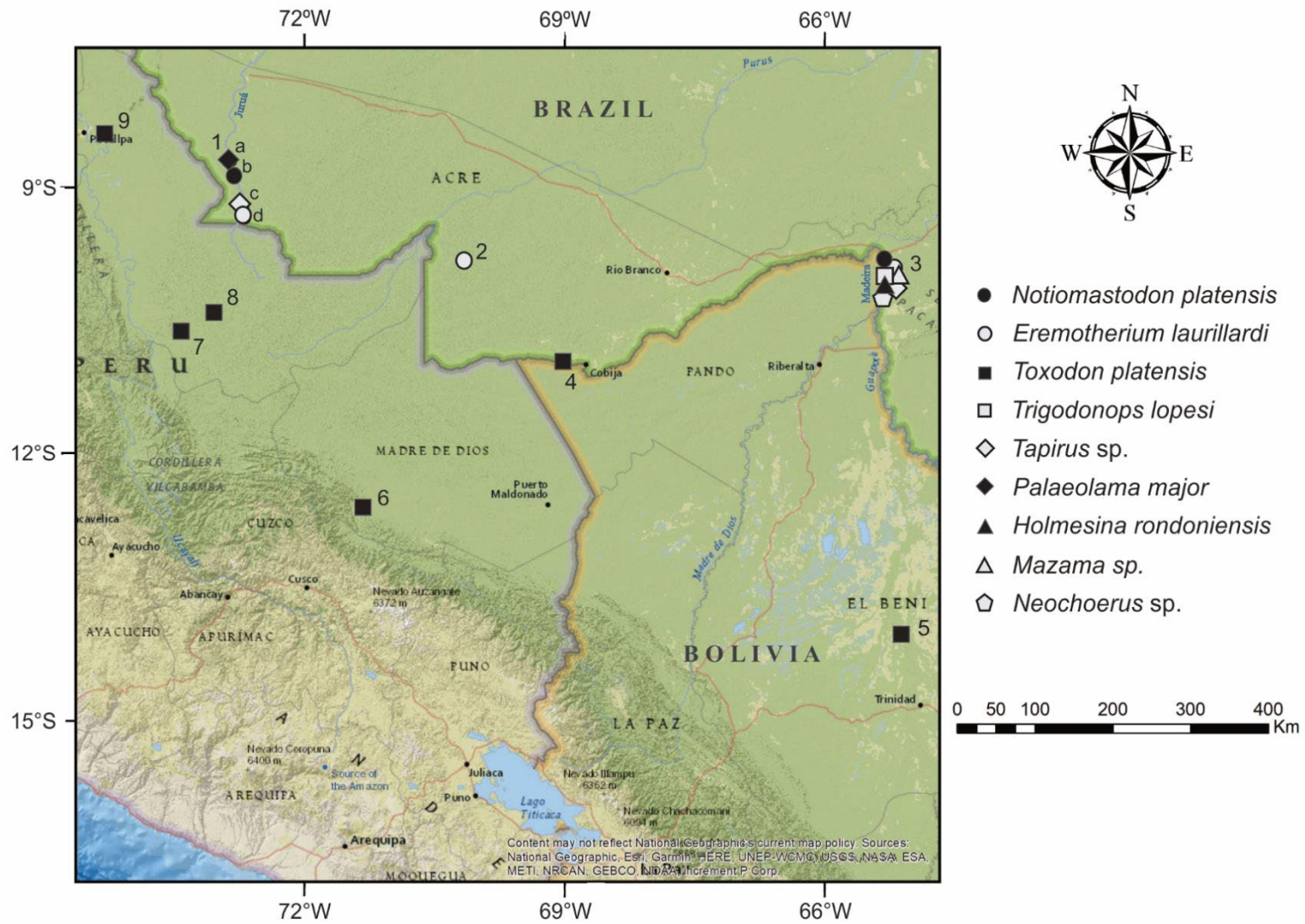
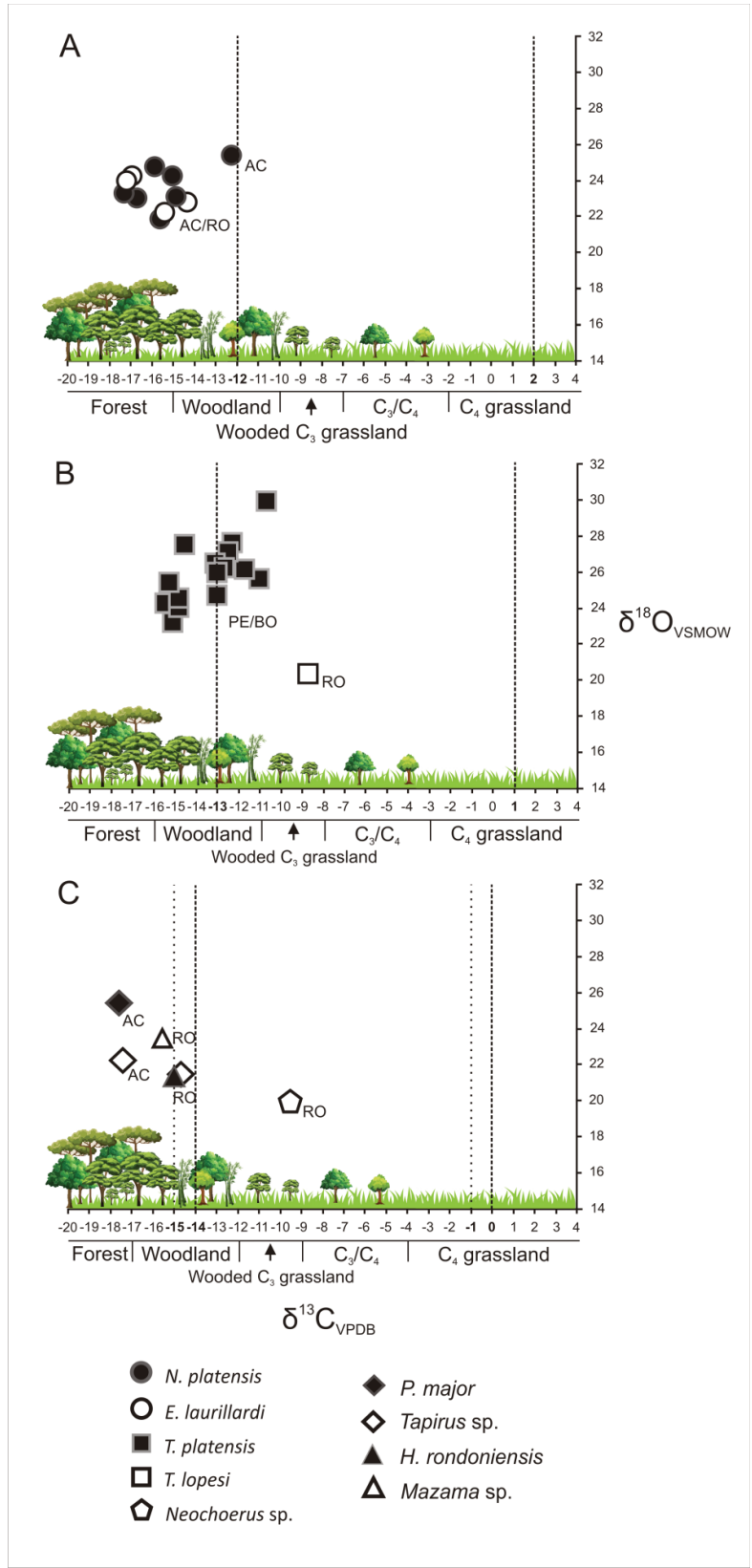
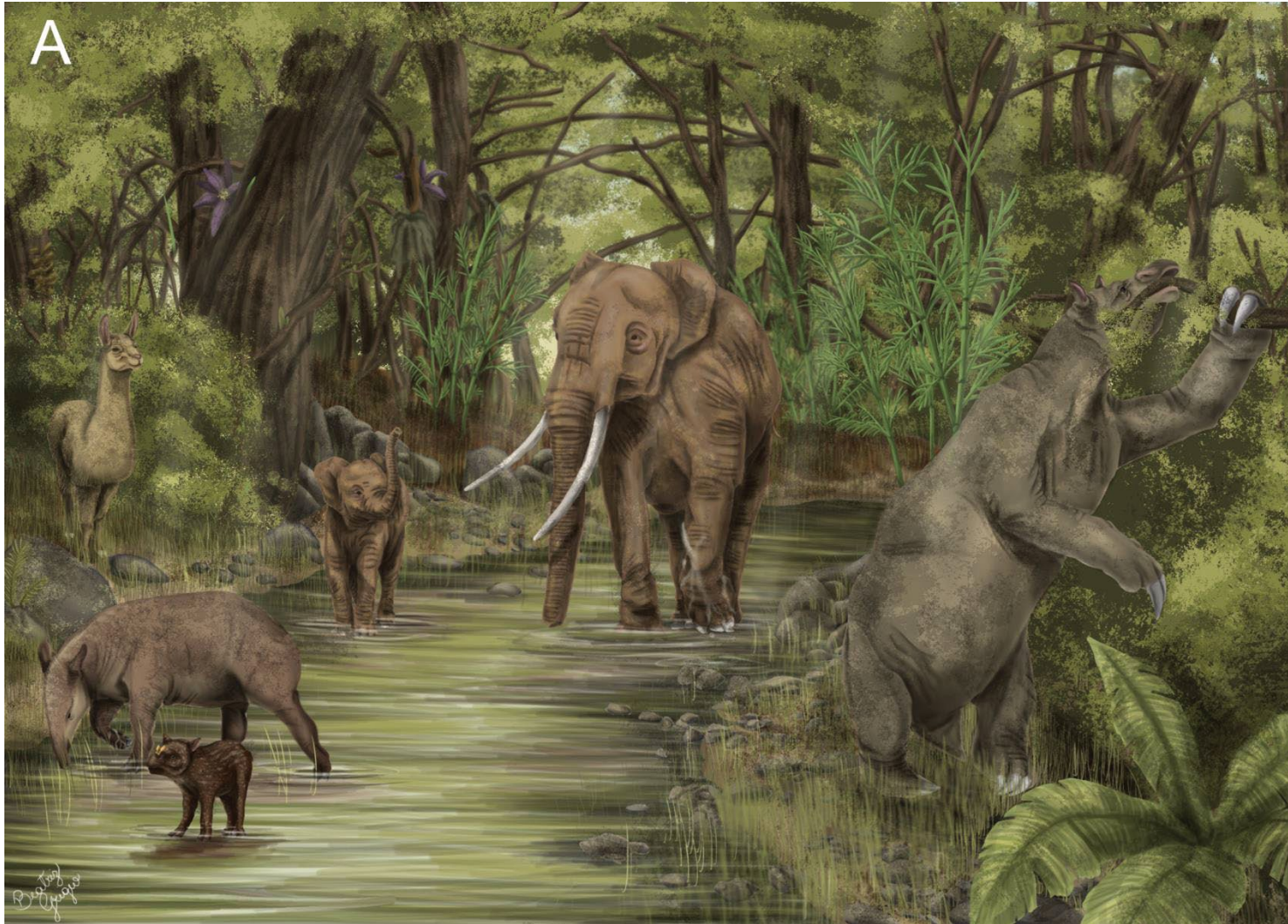


Fig. 1



**Fig. 2**



**Fig. 3A**

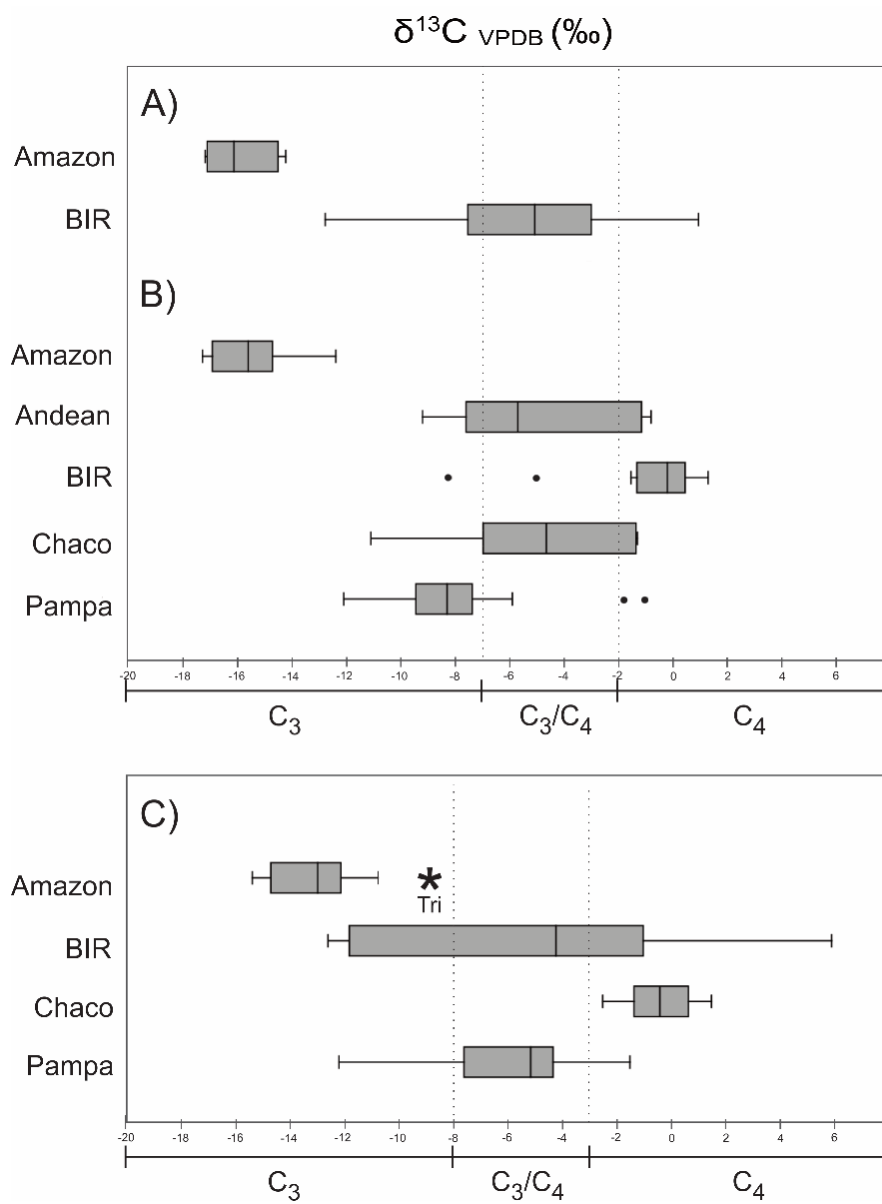




Fig. 3B



**Fig. 3C**



**Fig. 4**

**Table 1.**

<b>Species</b>	<b>BM (~Kg)</b>	<b>n</b>	<b><math>\delta^{13}\text{C}</math> ‰VPDB</b>	<b><math>p_i\text{C3}</math></b>	<b><math>p_i\text{C4}</math></b>	<b><math>B_A</math></b>	<b><math>\delta^{18}\text{O}</math> ‰VSMOW</b>
<b>A)</b>							
<i>E. laurillardii</i>	3,500 <sup>a</sup>	1	- 14.23	1.00	0.00	0.00	22.72
<i>N. platensis</i>	6,300 <sup>a</sup>	5	- 15.9 ± 1.2	1.00	0.00	0.00	23.07 ± 0.9
<i>T. lopesi</i>	1,900 <sup>b</sup>	1	- 8.83	0.70	0.30	0.72	20.29
<i>Tapirus</i> sp.	250 <sup>c</sup>	1	- 14.77	1.00	0.00	0.00	21.30
<i>H. rondoniensis</i>	120 <sup>a</sup>	1	- 14.89	1.00	0.00	0.00	21.37
<i>Nechoerus</i> sp.	200 <sup>d</sup>	1	- 9.66	0.69	0.31	0.75	19.90
<i>Mazama</i> sp.	40 <sup>e</sup>	1	- 15.47	1.00	0.00	0.00	23.57
<b>B)</b>							
<i>E. laurillardii</i>	3,500 <sup>a</sup>	3	- 16.5 ± 1.0	1.00	0.00	0.00	23.31 ± 1.1
<i>N. platensis</i>	6,300 <sup>a</sup>	2	- 14.1 ± 2.4	1.00	0.00	0.00	24.95 ± 0.5
<i>P. major</i>	280 <sup>a</sup>	1	- 17.47	1.00	0.00	0.00	25.80
<i>Tapirus</i> sp.	250 <sup>c</sup>	1	- 17.33	1.00	0.00	0.00	22.80
<b>C)</b>							
<i>T. platensis</i>	1,800 <sup>a</sup>	5	- 13.9 ± 1.6	≥ 0.86	≤ 0.14	≤ 0.32	25.11 ± 1.6
<b>D)</b>							
<i>T. platensis</i>	1,800 <sup>a</sup>	12	- 13.2 ± 1.4	≥ 0.84	≤ 0.16	≤ 0.38	26.05 ± 1.6

**Table 2.**

<b>Collection code</b>	<b>Locality</b>	<b><math>\delta^{18}\text{Op}\text{‰}</math></b>	<b><math>\delta^{18}\text{Ow}\text{‰}</math></b>
MERO ARQ 016	Madeira River, RO	14.46	-9.40
MERO PV 132 e 136	Madeira River, RO	14.73	-9.12
MERO PV 138	Madeira River, RO	12.96	-10.99
UFAC 1214	Madeira River, RO	14.21	-9.67
UFAC 4408	Madeira River, RO	15.51	-8.29
UFAC 104	Juruá River, AC	15.91	-7.86
UFAC PV 95	Juruá River, AC	16.58	-7.15

Supplementary Table 1.

Species	Collectioncode	Sample	Locality	$\delta^{13}\text{C} \text{‰VPDB}$	$\delta^{18}\text{O} \text{‰VSMOW}$	Calibrated Age ( $^{14}\text{C}$ )
<i>Notiomastodon platensis</i>	MERO ARQ 016	E	Araras, Madeira River, Nova Mamoré, Rondônia	-16.93	23.16	25,454 - 24,884
	MERO PV 132 e 136	E	Araras, Madeira River, Nova Mamoré, Rondônia	-17.29	23.43	
	MERO PV 138	E	Araras, Madeira River, Nova Mamoré, Rondônia	-15.61	21.66	
	UFAC PV 1214	E	Araras, Madeira River, Nova Mamoré, Rondônia	-14.72	22.91	
	UFAC PV 4408	E	Araras, Madeira River, Nova Mamoré, Rondônia	-14.95	24.21	
	UFAC PV 104	E	Pedra Preta, Juruá River, Acre	-15.83	24.61	
	UFAC PV 95	E	Pedra Preta, Juruá River, Acre	-12.39	25.28	
<i>Eremotherium laurillardi</i>	MERO PV 059	B	Araras, Madeira River, Nova Mamoré, Rondônia	-14.23	22.72	11,320 - 11,131
	UFAC PV 98	B	Arenal, Juruá River, Cruzeiro do Sul, Acre	-16.90	24.09	
	EL 06 s/cod	B	Juruá River, Acre	-17.19	23.77	
	UFAC PV 6450	B	ChandlersRiver, Acre	-15.37	22.07	
<i>Palaeolama major</i>	UFAC PV 061	D	Igarapé São Luis, Juruá River, Acre	-17.47	25.80	
<i>Tapirus</i> sp.	UFAC PV 035	B	Torre da Lua, Juruá River, Cruzeiro do Sul, Acre	-17.33	22.28	
<i>Homelsinarondoniensis</i>	MERO-P-002	B	Araras, Madeira River, Nova Mamoré, Rondônia	-14.89	21.37	
<i>Nechoerus</i> sp.	MERO (no code)	D	Araras, Madeira River, Nova Mamoré, Rondônia	-9.66	19.90	29,072 - 27,713
<i>Mazama</i> sp.	UFAC PV 4435B	B	Araras, Madeira River, Nova Mamoré, Rondônia	-15.47	23.57	
<i>Trigodonopslopesi</i>	MERO PV 100	D	Araras, Madeira River, Nova Mamoré, Rondônia	-8.83	20.29	

Species	Collectioncode	Sample	Locality	‰VPDB	$\delta^{18}\text{O}$ ‰VSMOW
<i>Toxodon platensis</i>	U-C1010	E	Beni-Yucuma-Maracas, Bolivia	- 11.00	
	U-C1011	E	Beni-Yucuma-Maracas, Bolivia	- 15.10	
	U-C1019-20	E	Beni-Yucuma-Maracas, Bolivia	- 14.70	
	U-C1012	E	Pando-Cobija, Bolivia	- 14.00	
	U-C1013	E	Pando-Cobija, Bolivia	- 14.50	
	U-C1018	E	Madre de Dios, Peru	- 13.00	
	F-04-001	E	InuyaRiver, Peru	- 12.50	
	F-04-002	E	InuyaRiver, Peru	- 10.70	
	F-04-003	E	InuyaRiver, Peru	- 12.70	
	F-04-004	E	InuyaRiver, Peru	- 11.70	
	F-04-005	E	PisquiRiver, Ucayali, Peru	- 15.30	
	F-04-006	E	Mapuya, Peru	- 12.30	
	F-04-007	E	Mapuya, Peru	- 13.00	
	F-04-008	E	Mapuya, Peru	- 12.80	
	F-04-009	E	Mapuya, Peru	- 15.40	
	F-04-010	E	Mapuya, Peru	- 14.10	
	F-04-011	E	Contamana, Peru	- 14.80	